Transient release of dopamine in response to rewarding stimulation of the medial forebrain bundle

Marie-Pierre Cossette

A Thesis

in

The Department

of

Psychology

Presented in Partial Fulfillment of the Requirements

for the Degree of Master of Arts (Psychology) at

Concordia University

Montreal, Quebec, Canada

August 2011

CONCORDIA UNIVERSITY

School of Graduate Studies

This is to certify that the thesis prepared

By: Marie-Pierre Cossette

Entitled: Transient release of dopamine in response to rewarding stimulation of the medial forebrain bundle

and submitted in partial fulfillment of the requirements for the degree of

Master of Arts (Psychology)

complies with the regulations of the University and meets the accepted standards with respect to originality and quality.

Signed by the final examining committee:

_____Dr. Andrew Chapman _____Chair

_____Dr. Wayne Brake_____Examiner

_____Dr. Nadia Chaudhri_____Examiner

_____Dr. Peter Shizgal_____Supervisor

Approved by _____Dr. Wayne Brake_____
Chair of Department or Graduate Program Director

_____20___ _____Brian Lewis_____
Dean of Faculty

ABSTRACT

Reward valuation is a core computation that guides appetitive behaviour. Intracranial self-stimulation (ICSS) is among the principal behavioural tools employed to study neural correlates of reward seeking. The current thesis investigated anatomical and functional neural components subserving ICSS of the medial forebrain bundle (MFB), with particular attention to the mesolimbic dopamine (DA) pathway.

The axons of midbrain DA neurons course through the MFB, and MFB stimulation produces transient DA release in terminal fields. However, the mechanism responsible for DA activation and the precise function of phasic DA activity in ICSS are still disputed. In Experiment 1, DA transients were measured in the nucleus accumbens (NAc) shell by means of fast-scan cyclic voltammetry (FSCV). Unilateral MFB stimulation drove DA transients in both hemispheres. Given that the DA projection to the NAc is almost exclusively unilateral, the contralateral transients are attributed to trans-synaptic activation of the DA neurons. A disynaptic route entailing a pontine relay provides a plausible route by which excitation in non-DA MFB fibers can reach DA cell bodies in the contralateral hemisphere, and a combination of monosynaptic and disynaptic routes may funnel such excitation to ipsilateral DA neurons.

Experiment 2 assessed the hypothesis that midbrain DA neurons either perform spatio-temporal integration of synaptic input from directly activated MFB fibers subserving ICSS or relay the results of such integration to efferent stages of the reward

circuitry. Current-frequency trade-off functions were derived from curves relating the stimulation current to ICSS performance or to the amplitude of NAc DA transients. Whereas the behaviourally derived trade-off functions decline monotonically as a function of pulse frequency, the trade-off functions derived from DA transients driven by the same electrodes are either U-shaped or level off as the pulse-frequency is increased. The contrast between the two sets of trade-off functions is inconsistent with the hypothesis that DA neurons projecting to the NAc shell constitute an entire series stage of the neural circuit subserving self-stimulation of the MFB.

ACKNOWLEDGEMENTS

I first want to express all my gratitude to Dr. Shizgal for his guidance and trust. I feel privileged to be under his constructive supervision, which, in challenging me, ensured that I made consistent and constant progress. I thank my committee members for taking the time to review my thesis and I look forward for their valuable feedback on my work. The contribution of David Munro and Christophe Lower for technical support was essential for the completion of the work presented here. They have been fantastic and very supportive.

I want to thank all the people at the CSBN for making the working environment such a great place. They managed to put a smile on my face everyday. A particular mention must be made of several individuals: Giovanni Hernandez, who taught me so much, not only in terms of technique but also critical thinking, Suzanne Hood, who I consider a model of integrity, professionalism and kindness, Brian Dunn, who not only helped me with numerous pieces of writing including this thesis but also for his incredible insights about life and human nature, and Ivan Trujillo, for his enthusiasm for science and his rigorous scientific thinking. I could not have asked for better mentorship. Finally, I want to thank my family who taught me to have confidence in my abilities and to persevere when it really matters. Their presence in my life provides the comfort, security and love that makes everything else possible.

TABLE OF CONTENTS

LIST OF FIGURES: Experiment 1

LIST OF FIGURES: Experiment 2

LIST OF ABBREVIATIONS

ChAT	Choline acetyltransferase
ChR2	Channelrhodopsin-2
DA	Dopamine
DAT	Dopamine transporter
eNpHR	Enhanced halorhodopsin
FSCV	Fast-scan cyclic voltammetry
Glu	Glutamate
ICSS	Intracranial self-stimulation
LDTg	Laterodorsal tegmental nucleus
LH	Lateral hypothalamus
LPOA	Lateral preoptic area
MFB	Medial forebrain bundle
MPFC	Medial prefrontal cortex
NAc	Nucleus accumbens
PPTg	Pedunculopontine tegmental nucleus
SLEA	Sublenticular extended amygdala
VTA	Ventral tegmental area
VP	Ventral pallidum

GENERAL INTRODUCTION

Goal-directed behaviours permeate every sphere of life, allowing us to plan actions to obtain goal objects necessary for survival, growth, reproduction, and defense. Goal objects capable of sustaining approach behaviours are called rewards. To allocate resources appropriately, payoffs for the available options must be estimated, an operation that must take into account reward value, cost, and risk (Shizgal, 1997). Thus, reward valuation is a core computation that guides appetitive behaviour. A wide spectrum of behaviours can serve to procure desirable goal objects, both those that occur naturally, and artificial ones, such as drugs or rewarding electrical stimulation. Such instrumental approach behaviours are thought to arise from the activity of common neural pathways, regardless of the kind of rewards that are sought (Beyene, 2009; Ikemoto, 2010). If so, deepening our understanding of the neural circuitry subserving artificial laboratory rewards should shed light on neural mechanisms crucial for adaptive behaviours in the natural environment.

Intracranial self-stimulation (ICSS) is among the principal behavioural tools employed to study brain reward circuitry. Rats and other vertebrates will work vigorously to trigger electrical stimulation, particularly when the stimulating electrodes are located along the trajectory of the medial forebrain bundle (MFB) (Olds & Olds, 1963). Electrical stimulation can compete or summate with natural reinforcers, suggesting that the phenomenon of ICSS is produced by inducing a neural signal in the reward circuitry that is evaluated similarly to natural goal objects (Conover & Shizgal, 1994; Conover, Woodside & Shizgal, 1994) and thus, is capable of eliciting reward seeking.

Mesolimbic dopamine (DA) neurons have long been implicated in ICSS (Crow, 1970; Wise, 1978). For example, narcoleptics block or reduce responding for ICSS whereas indirect DA agonists, such as amphetamine and cocaine, potentiate responding for ICSS (Gallistel & Karras, 1984; Wise, 2004). Although the contribution of DA neurotransmission to the rewarding effects of MFB stimulation is widely accepted, no consensus has been reached on how DA neurons are recruited by the stimulating electrode nor on the exact function DA neurotransmission serves in ICSS (Hernandez, Breton, Conover & Shizgal, 2010).

Three activity states have been described in DA neurons: quiescence; slow, steady ("tonic") firing; and burst ("phasic") firing (Grace, Floresco, Goto & Lodge, 2007). Tonic firing maintains a steady-state extracellular concentration of DA in terminal fields and is dependent on the proportion of DA somata in the quiescent ("off") state (Grace & Bunney, 1984a; Floresco, West, Ash, Moore & Grace, 2003). In contrast, phasic firing consists of bursts of at least 2 or 3 spikes and is time-locked to specific external or internal stimuli (Grace & Bunney, 1984b; Grace & Onn, 1989, Hyland, Reynolds, Hay, Perk & Miller, 2002). These phasic bursts produce transient increases in the extracellular concentration of DA (Gonon, 1988; Wightman, Amatore, Engstrom et al, 1988; Kawagoe & Wightman, 1994; Kilpatrick, Rooney, Micheal & Wightman, 2000).

Cell bodies of midbrain DA neurons are located in the ventral tegmental area (VTA)-substantial nigra complex and project widely throughout the brain. Based on these projections, DA cell bodies have been grouped into three distinct pathways, anatomically and functionally: the mesocortical, mesostriatal and mesolimbic pathways (Bjorklund & Dunnett, 2007). The mesolimbic connections, especially the ones sending

input from the posteromedial VTA to the medial nucleus accumbens (NAc) shell, are implicated strongly in goal-directed behaviours such as drug self-administration (Ikemoto, 2010). Furthermore, pharmacological manipulations of DA activity in the NAc shell projections are particularly efficient at modulating performance levels for ICSS compared to when these manipulations target the NAc core or the dorsal striatum. For this reason, several ICSS studies investigating the neural correlates of reward seeking have focused their attention on DA activity in the VTA-NAc shell projection, which was chosen as the target structure for the experiments described here.

This thesis will focus on phasic firing of midbrain DA neurons and the resulting DA transients that rewarding MFB stimulation triggers in the shell region of the NAc terminal field. The first experiment questions the mechanism by which midbrain DA neurons are activated. DA axons do course near the tip of the stimulation electrode (Ungerstedt, 1971), and it has been argued that these axons are recruited directly by the electrical stimulation (German & Bowden, 1974; Corbett & Wise, 1980). However, the fine, unmyelinated axons of DA neurons have high thresholds to activation by extracellular currents. Behavioural studies implicate more excitable, myelinated neurons in the rewarding effect of MFB stimulation (Shizgal, Biejalew, Corbett, Skelton & Yeomans, 1980; Biejalew & Shizgal, 1982, Biejalew & Shizgal, 1986), and electrophysiological studies have identified non-DA neurons driven by MFB stimulation that have characteristics consistent with those inferred from the behavioural studies (Rompré & Shizgal, 1986; Shizgal, Schindler & Rompré, 1989, Murray & Shizgal, 1996). Given evidence that at least some of the directly activated neurons subserving MFB self-stimulation project in the descending direction, it has been suggested

(Yeomans, Kofman & McFarlane, 1985; Yeomans, 1989; Murray & Shigal, 1994; Shizgal et al., 1980; Wise, 1980) that DA (or other monoaminergic) neurons may be activated trans-synaptically by non-DA fibers directly recruited by the rewarding stimulation. Such trans-synaptic activation has been demonstrated electrophysiologically (Maeda & Mogenson, 1981).

Yet another mechanism by which DA neurons may be recruited by rewarding MFB stimulation is implied by demonstrations that dopamine release is elevated bilaterally in response to electrical stimulation (Phillips, Jakubovic, & Fibiger, 1987; Garrigues & Cazala, 1983; Nakahara, Fuchikami, Oazi, Iwaski & Nagatsu, 1992). Anatomical studies show that DA neurons in the ventral midbrain project almost exclusively to the ipsilateral hemisphere (Lindvall & Björklund, 1974; Swanson, 1982; Ikemoto, 2007). Thus, contralateral DA activation is consistent with a trans-synaptic route. Anatomical work discussed below (Experiment 1) suggests that this route is disynaptic and involves a pontine relay. Thus, three different routes have been proposed to link rewarding MFB stimulation to the DA transients it evokes in the NAc terminal field: direct activation of DA fibers, monosynaptic activation of DA somata by descending MFB fibers directly recruited by the stimulation, and disynaptic activation via a pontine relay. All three routes may contribute to DA transients in the same hemisphere as the stimulation electrode, but only the disynaptic route is expected to generate DA transients in the contralateral hemisphere. In Experiment 1, DA transients evoked by rewarding MFB stimulation were measured in both the ipsilateral and contralateral hemispheres.

As a step toward linking the different neural elements of the reward circuitry to the psychological processes they subserve, Experiment 2 focused on the role of phasic DA activity in the rewarding effect of ICSS. It has been demonstrated that the reward efficiency of the electrical stimulation is dependent on the spatio-temporal integration of the action potentials triggered at the tip of the electrode (Gallistel, 1978; Simmons & Gallistel, 1994; Gallistel, Shizgal & Yeomans, 1981). In this view, neurons implicated in computing the strength of the reward signal act as a monotonic counter, producing the same output in response to a given number of incident action potentials, regardless of whether this "count" arises from stimulating many neurons at a low pulse frequency or from stimulating fewer neurons at a higher pulse frequency. This relationship between pulse frequency and current is expressed in a trade-off function derived from ICSS performance. The current required to meet a behavioural criterion, such as half-maximal performance, is measured as a function of the pulse frequency. The current determines the number of stimulated neurons whereas the pulse frequency determines the number of times each stimulated neuron fires during a stimulation train. As predicted by the counter model of spatio-temporal integration, the current-frequency trade-off functions reflect the form predicted by the counter model of spatio-temporal integration in the neural substrate for ICSS (Gallistel, 1978, Gallistel, Shizgal & Yeomans, 1981; Forgie and Shizgal, 1993; Simmons & Gallistel, 1994) .

Performance for rewarding MFB stimulation increases as a monotonic function of the current, pulse duration, and pulse frequency (Gallistel, 1978). These findings serve as the foundation for experiment 2, because they imply that all stages of the neural circuitry that intervene between the stimulation electrode and the observed behavioural response

behave monotonically over the tested ranges of the stimulation parameters. The logic leading to this conclusion was first described by Gallistel and colleagues (1981). If the output of the last stage of the reward valuation process that generates ICSS performance is monotonic, then holding its output constant (by imposing a behavioural criterion) also holds constant its input. Any other shape in the function relating the behaviour output of the last stage as a function of its input would result in ambiguity and loss of information (see Figure 1). For instance, if the function resembled an inverted U, each behavioural output could arise from two different inputs (arrayed along the ascending and descending portions of the inverted U). Such a non-monotonic relationship would necessarily be expressed in the behavioural output. The monotonic dependence of ICSS performance on the basic stimulation parameters demonstrates that such loss of information does not occur over the tested ranges of the inputs. Such results can be obtained only if monotonicity is preserved throughout all the stages that link excitation at the tip of the electrode to the observable behavioural output. This logic is the basis for the test performed in Experiment 2, to determine whether phasic signalling in mesolimbic DA neurons can constitute an entire series stage of the pathway responsible for MFB self-stimulation.

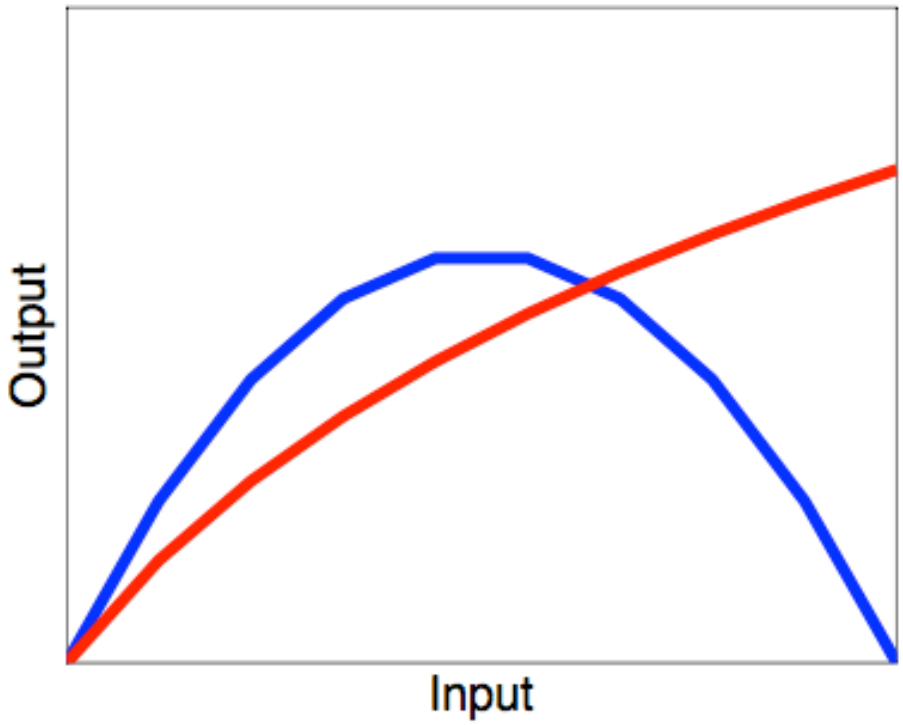

Figure 1. Hypothetical input-output functions for a given stage of reward valuation. In the case of the monotonic function (red line) each output is produced by only one specific input. Consequently, holding the output constant (e.g., by imposing a behavioural criterion) also holds constant its input. In the case of the non-monotonic function (blue line) each behavioural output could arise from two different inputs, arrayed along the ascending and descending portions of the inverted U. This will produce a loss of information that cannot be recovered in subsequent stages.

It has been proposed that midbrain DA neurons a) perform the spatio-temporal integration of the synaptic potentials generated by impulse flow in directly stimulated neurons responsible for the rewarding effect of MFB stimulation or b) relay the integrated reward signal to efferent stages of the reward pathway (Moisan & Rompré, 1998). If so, the midbrain DA neurons function as a series stage in this pathway. Given the required monotonicity across all stages of reward processing, if the activity of DA neurons track the aggregate impulse flow, they must display a current-frequency trade-off function consonant with the one derived from ICSS performance.

In Experiment 2, current-frequency trade-off functions were derived, both from ICSS performance and from stimulation-induced DA transients recorded in the NAc. The trade-off functions were compared to test the plausibility of the Moisan & Rompré model, and thus to shed light on the role of phasic DA activity in the rewarding effect of MFB stimulation.

EXPERIMENT 1

INTRODUCTION

ICSS is among the principal behavioural tools employed to study brain reward circuitry. Performance for ICSS is particularly robust when the stimulating electrodes are located along the trajectory of the MFB (Olds & Olds, 1963). Manipulation of dopaminergic neurotransmission systematically alters performance for rewarding stimulation of the MFB (Fouriezos et al., 1978; Franklin, 1978; Gallistel and Karras, 1984; Bauco and Wise, 1997; Colle and Wise, 1988; Crow, 1970; Gallistel and Karras, 1984; Hernandez et al., 2010). Single pulse trains targeted to the MFB drive transient release of DA in the NAc terminal field (Gratton, Hoffer & Gerhardt, 1988; Gonon, 1988; Wightman et al., 1988; Kawagoe & Wightman, 1994), and repeated trains produce long-lasting increases in the extracellular concentration of DA in the NAc (Nakahara, Ozaki, Kapoor, & Nagatsu, 1989; Nakahara, Fuchikami, Ozaki, Iwasaki & Nagatsu, 1992; Fiorino, Coury, Fibiger, & Phillips, 1993). Although the axons of midbrain DA neurons course through ICSS sites along the MFB, consensus has not been reached concerning the mechanisms responsible for the activation of these neurons by MFB stimulation, or about the precise role played by these neurons in ICSS (Hernandez, et al., 2010).

The MFB contains at least 50 different types of fibers (Nieuwenhuys, Geeraedts & Veening, 1982; Veening, Swanson, Cowan, Nieuwenhuys & Geeraedts, 1982) of

different origin and destination. The potential mechanisms by which midbrain DA neurons can be activated during MFB stimulation are numerous (see Figure 2), but can be grouped as three types: direct, monosynaptic and disynaptic (see Figure 3). In this view, the stimulation electrode can produce action potentials directly in the ascending DA axons. The stimulation can also recruit non-DA fibers descending through the MFB that synapse onto the VTA, and descending through the MFB that project to an intermediate group of neurons (e.g., laterodorsal tegmentum) that in turn, synapse onto the VTA.

The first type of DA activation, the direct one, is at the core of a long-standing view that activation of DA axons in the MFB at the level of the lateral hypothalamus (LH) is the predominant cause for DA release at the terminals (German & Bowden, 1974; Corbett & Wise, 1980). Early reports showed that the density of DA fibers near the tip of the stimulating electrode correlates with low threshold for MFB ICSS and more vigorous response rate.

However, electrophysiological studies have demonstrated that MFB stimulation also recruits non-DA neurons (Rompré & Shizgal, 1986; Shizgal, et al., 1989; Murray & Shizgal, 1996). Estimates of conduction velocity, recovery from refractoriness, and the behaviourally relevant direction of conduction in these non-DA neurons differ from the characteristics of DA axons (Shizgal et al., 1980; Biejalew & Shizgal, 1982, Biejalew & Shizgal, 1986). These studies are in line with the second and third types of DA excitation proposed above, namely monosynaptic and disynaptic activation.

In order for MFB stimulation to both directly and indirectly activate VTA DA neurons, charge density must be sufficiently high at the electrode tip to excite the fine,

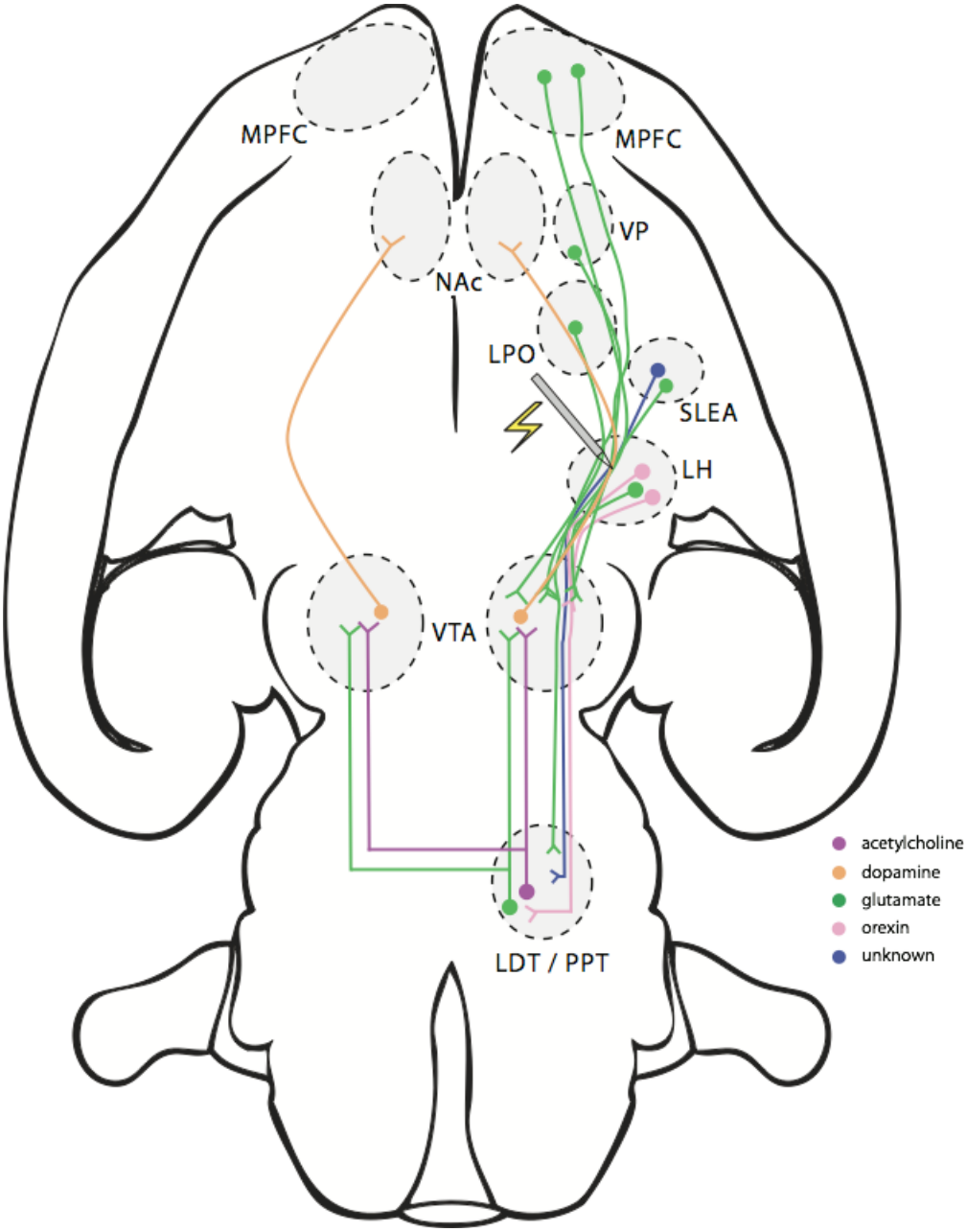

Figure 2. The heterogeneity of the medial forebrain bundle at the level of the lateral hypothalamus. Only a small subset of the 50+ populations of MFB fibers is shown. Figure prepared by Ivan Trujillo and Peter Shizgal (personal communication).

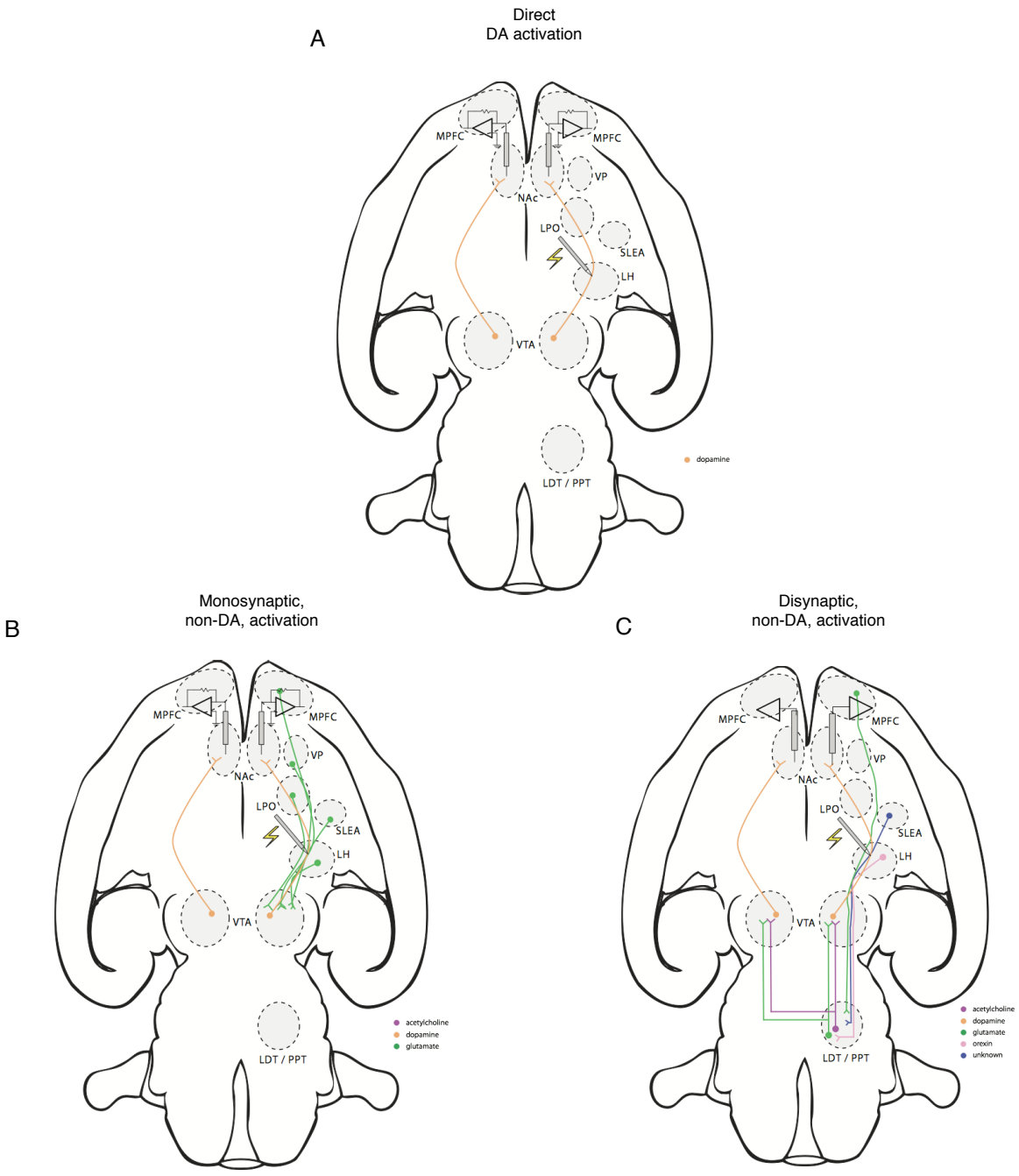
A
Direct
DA activation
MPFC
MPFC
VP
NAc
LPO
SLEA
LH
VTA
LDT / PPT
dopamine
B
Monosynaptic,
non-DA, activation
MPFC
MPFC
VP
NAc
LPO
SLEA
LH
VTA
LDT / PPT
acetylcholine
dopamine
glutamate
C
Disynaptic,
non-DA, activation
MPFC
MPFC
VP
NAc
LPO
SLEA
LH
VTA
LDT / PPT
acetylcholine
dopamine
glutamate
orexin
unknown

Figure 3. Possible route of DA activation. A) Direct activation of the ascending DA axons. B) Monosynaptic activation: Descending, non-DA, MFB fibers are activated directly by the stimulation. These fibers provide excitatory synaptic input to VTA DA neurons. C) Disynaptic activation: Descending, non-DA, MFB fibers are activated directly by the stimulation. These fibers provide excitatory synaptic input to neurons in the laterodorsal tegmental nucleus and pedunculopontine nucleus, which, in turn, provide excitatory synaptic input to VTA DA neurons in both hemispheres. Figure prepared by Ivan Trujillo and Peter Shizgal (personal communication).

unmyelinated DA axons (Yeomans, 1989). Although the case for indirect activation of DA somata by MFB stimulation has long been established (Rompré & Shizgal, 1986; Shizgal, et al., 1989; Murray & Shizgal, 1996; Shizgal et al., 1980; Biejalew & Shizgal, 1982, Biejalew & Shizgal, 1986; Sombers, Beyene, Carelli & Wightman, 2009), the relative contribution of direct (axonal) and indirect (trans-synaptic) activation to stimulation-induced release of DA has not.

Three activity states have been described in DA neurons: quiescence; slow, steady ("tonic") firing; and burst ("phasic") firing (Grace, et al., 2007). Tonic firing maintains a steady-state extracellular concentration of DA in terminal fields. This concentration varies with the proportion of DA somata in the quiescent ("off") state (Grace & Bunney, 1984a; Floresco et al., 2003). Superimposed on the steady background firing are phasic bursts consisting of at least 2 or 3 spikes at an average intra-burst frequency of 20 hertz (Grace & Bunney, 1984b; Grace & Onn, 1989; Hyland et al., 2002). These phasic bursts produce transient increases in the extracellular concentration of DA (Gonon, 1988; Wightman, Amatore, Engstrom et al, 1988; Kawagoe & Wightman, 1994; Kilpatrick, Rooney, Micheal & Wightman, 2000). Changes in burst firing occur rapidly and are time-locked to specific external or internal stimuli.

Basal levels of DA can be measured by content analysis of tissue samples and microdialysis. Transient changes in DA release, in contrast, are tied to burst firing induced by specific events. Their measurement requires techniques designed for fast sampling, on the scale of milliseconds. To better examine the routes of DA activation triggered during MFB ICSS, fast-scan cyclic voltammetry (FSCV) was used in this experiment to measure changes in DA transients time-locked to the electrical stimulation.

This technique is well-suited to detecting DA transients because of its high temporal resolution (one measure every 100 ms).

Several lines of evidence suggest that MFB stimulation produces changes in DA release in the NAc bilaterally. Fos expression in response to the electrical stimulation of MFB is observed in both the ipsi- and the contralateral VTA and the NAc (Hunt & McGregor, 1998; Arvanitogiannis, Flores, Pfaus, & Shizgal, 1996; Nakahara, Ishida, Nakamura, Kuwahara, Todoka & Nishimori, 1999). Samples obtained from terminal-field tissue punches revealed increases in DA levels in both hemispheres (Phillips, Jakubovic, & Fibiger, 1987; Garrigues & Cazala, 1983). Nakahara and colleagues (1992) used microdialysis to measure DA levels in the NAc following MFB stimulation and observed bilateral increases. Because midbrain DA projections are overwhelmingly unilateral (Lindvall & Björklund, 1974; Swanson, 1982; Ikemoto, 2007), contralateral changes in DA activation during MFB stimulation most likely entail a trans-synaptic activation of the DA fibers. Because this is the case, the contralateral changes in DA activity provide a privileged window into the effects of indirect DA activation in isolation. In contrast, changes in DA release ipsilateral to the stimulation site could reflect all three mechanisms for activating DA neurons: direct, monosynaptic and disynaptic.

Monosynaptic and disynaptic DA activation during MFB stimulation could arise in multiple ways (see Figure 3b and 3c). Forebrain glutamatergic neurons and pontine cholinergic neurons are good candidates for linking MFB stimulation to trans-synaptic DA activation.

Glutamatergic neurotransmission has been linked to reward seeking. Glutamate (Glu) agonists injected intra-VTA induce phasic activity in DA neurons (Chergui, Charlety, et al., 1993; Overton & Clark, 1992) and produce DA transients as recorded by FSCV in the NAc (Sombers, et al., 2009). Furthermore, Glu receptor antagonists infused in the VTA modulate changes in DA release during laterodorsal tegmental nucleus (LDTg) stimulation, as measured by chronoamperometry (Forster & Blaha, 2000). MFB stimulation also triggers changes in tonic levels of glutamate in the VTA (You, Chen & Wise, 2001). Behaviourally, pharmacological manipulations of glutamate release in the VTA alter levels of VTA ICSS (Sombers, 2009) or MFB ICSS (Herberg & Rose, 1990).

Cholinergic activity is also overwhelmingly implicated in reward seeking. Manipulations of the LDTg and PPTg, a region that sends afferents to the VTA, produce gradual changes in DA release in the NAc that are mediated, at least in part, by cholinergic neurotransmission (Forster & Blaha, 2000; Blaha & Phillips, 1996; Grace, et al., 2007; Yeomans, Mathur, Tampakeras, 1993; Yeomans, Forster & Blaha, 2001). In addition, manipulations of cholinergic neurotransmission in the VTA alter the stimulation strength required to sustain MFB ICSS (Yeomans et al., 1985; Yeomans & Baptista, 1997; Yeomans et al., 2000; Yeomans, et al., 2001).

There are multiple sources of glutamatergic input to the VTA, several of which arise in nuclei that send descending projections through the MFB. Combining unilateral injection of a retrograde tracer into the VTA and in situ hybridization for the vesicular glutamate transporter, VGLUT2, Geisler and colleagues (2007) found co-localization of the tracer and the glutamate marker in the medial prefrontal cortex (MPFC), the lateral preoptic area (LPOA), the ventral pallidum (VP), the sublenticular extended amygdala

(SLEA), and the LH, including the area of MFB targeted by the stimulating electrode in our ICSS preparation. All these projections were observed bilaterally, but were more pronounced in the ipsilateral hemisphere. However, it is unknown whether the decussation of these projections occurs at a point anterior or posterior to the stimulating electrode. For simplicity, it will be assumed that this possible monosynaptic activation, via Glu projections to the VTA, is restricted to the DA fibers ipsilateral to the stimulation site.

Geisler et al. (2007) also reported a bilateral, glutamatergic projection from the pedunculopontine tegmental nucleus (PPTg) /LDTg with comparable staining in both sides of the brain. Other anatomical reports provided evidence that LH projections synapse onto the PPTg/LDTg bilaterally, although less staining was reported in the contralateral hemisphere (Satoh & Fibiger, 1986; Steinenger, Rye & Wainer, 1992; Semba & Fibiger, 1992). The neurotransmitter released by these neurons has not been characterised unambiguously. Nevertheless, it is possible that a glutamatergic pathway could indirectly activate DA neurons via a projection coursing through the MFB and terminating in the PPTg/LDTg, which in turn would project to the VTA bilaterally. These connections include both glutamatergic fibers, identified via staining for VGLUT2, and cholinergic fibers, identified either via staining for acetylcholinesterase (a marker that has been shown to be only partially selective for cholinergic terminal regions in the central nervous system; (Bernard, Legay, Massoulie & Bloch, 1995)) or via the more specific marker, choline acetyltransferase (Geisler, Derst, Veh & Zham, 2007; Satoh & Figiber, 1986; Oakman, Faris, Kerr, Cozzari & Hartman, 1995). Such disynaptic activation could

recruit DA fibers in both hemispheres and could account for bilateral changes in DA activity during MFB stimulation (Yeomans, et al., 1993).

Anatomical studies strongly suggests that, if DA transients during MFB stimulation are observed in the contralateral side, they would depend solely on disynaptic DA activation. In the ipsilateral NAc, DA transients could be produced by three possible types of DA activation and thereby, are expected to grow more rapidly with increasing current when compared with DA transients measured in the NAc contralateral to the stimulation electrode.

The present experiment examined if rewarding MFB stimulation drives bilateral DA transients in the NAc, as measured by FSCV. The MFB stimulation was delivered at pulse durations of 0.1 and 2 ms. The lower value is employed typically in ICSS experiments, whereas FSCV experiments more commonly use the higher value. By including pulse durations of 0.1 ms and 2 ms, and stimulating over a wide range of currents, the results can help bridge findings obtained in these two types of experiments.

DA transients were observed bilaterally in all subjects and the current thresholds for these transients did not differ across hemispheres, for either pulse duration. Moreover, the growth of DA transients was steeper in the ipsilateral hemisphere. These findings are consistent with the trans-synaptic activation of midbrain DA neurons by descending MFB axons, and demonstrate that indirect activation plays a major role in producing phasic DA release during MFB stimulation, a more substantial role than previously acknowledged.

METHODS

Subjects

Subjects were 7 Long Evans male rats (Charles-River, St. Constant, QC, Canada). Animals weighed 300–350 g at their arrival. They were housed individually with ad libitum access to food and water and maintained on a 12 h light/dark reverse cycle (lights off from 08:00 to 20:00). The experimental procedures were performed in accordance with the principles outlined by the Canadian Council on Animal Care.

Intracranial self-stimulation

Surgery

In a first surgery, rats were anesthetized with a mixture of Ketamine hydrochloride (87 mg/kg) and xylazine hydrochloride (13 mg/kg). An s.c. injection of atropine sulphate was given to reduce bronchial secretions (0.05 mg/kg), an s.c. injection of buprenorphine to alleviate pain pre and post operation (0.05 mg/kg), and an s.c. injection of penicillin procaine to prevent infection (0.3 cc/rat). The animal's nose was placed in an isoflurane nose cone so that gas anesthetic could be administered continuously throughout the surgery (0.5 to 1.5%). One stimulating electrode, fashioned from 0.25 mm stainless steel insect pin and insulated with Formvar enamel to within 0.5 mm of the tip, was stereotaxically aimed at the right LH level of the MFB (AP: -2.8 mm; ML: 1.7 mm; DV: 8.9 mm from the skull; all coordinates are referenced to bregma). An additional electrode was placed in the external plexiform layer of the olfactory bulb (AP: 6.2 mm; ML: -0.1

mm; DV: 5 mm from the skull, all coordinates are referenced to bregma) to serve as the anode of the stimulation circuit. The location of the anode was chosen so as to place the recording site mid-way between the cathode and anode of the stimulation circuit. At that position, the recording site should lie on or near a zero-potential surface, thus reducing interference between the electrical stimulation and the voltammetric measurements.

The electrode assembly was secured with dental acrylic and anchored with jeweller's screws. The skull above the NAc was temporarily covered with bone wax, and two stainless steel tubes were positioned to guide the levelling of the head during the second surgery, the one performed prior to FSCV recordings.

Behavioural Measures

Upon recovery from the surgery, each animal was shaped to lever press for a 500 ms train of cathodal, rectangular, constant-current pulses with a pulse duration of 0.1 ms. Shaping took place in a Plexiglas operant chamber (30 cm long × 21 cm wide × 51 cm high) equipped with one retractable lever and a cue light positioned 1.5 cm above the lever. Illumination of the cue light signals that the lever press has been registered by the data acquisition system. A house light signalled the whole duration of the 10-s intertrial intervals. Each trial consisted of a fixed time during which the stimulation parameters were held constant. After completion of the work requirement, as determined by the price variable (see below), the lever was retracted for 2 s before being available again for lever pressing.

The reward efficacy of the MFB stimulation cathode was determined by means of behavioural testing; as described below, all MFB electrodes used in subsequent FSCV recordings were shown previously to support ICSS.

The behavioural measure was time allocation, the proportion of trial time during which the animal worked for the electrical stimulation. Time allocation was corrected as described in Breton, Marcus & Shizgal (2009). The stimulation frequency was held constant during a trial and was decremented systematically from trial to trial, in equal proportional steps. Trial time (the total time that the lever was extended) was 80 s, thus allowing the rat to harvest a maximum of 20 rewards at each pulse frequency. The range of frequencies tested was selected so as to describe the sigmoidal relationship between pulse frequency and time allocation. Ideally, three data points were positioned along the upper asymptote, three along the lower, and three on the rising portion.

Initially, rats were trained to depress the lever for a cumulative period of 1 s, referred to as the price of a stimulation train. If the rat displayed signs of aversion or excessive motor effects, it was excluded from the experiment. After the rats performed well for trains offered at the 1-s price, the price was increased gradually to 4 s. Training continued daily until the behaviour was stable over five consecutive sessions. Successful completion of the behavioural training was a proxy to determine that the MFB electrodes produced a sufficiently potent rewarding effect to be used in the voltammetric preparation.

Fast-scan cyclic voltammetry

Surgery

Rats were anesthetized with urethane (1.5 g/kg) and placed in the stereotaxic frame (Kopf Instrument, Tujunga, CA). The bone wax was removed and the head levelled with reference to the two guides tubes. The animal's temperature was constantly monitored and controlled with a thermal pad. A carbon-fiber electrode, pre-cleaned with 2-propanol containing activated carbon, was slowly lowered into the NAc shell (AP: 1.7 mm; ML: 1.0 mm; DV: 7 mm from the skull). A sintered Ag/AgCl reference electrode (In vivo metrics, Healdsburg, CA) was placed in the hemisphere contralateral to the carbon fiber, on or near the zero potential surface of the electrical field around the stimulation current. MFB stimulation trains (2 ms pulse duration, 500 μA, 60 Hz) were delivered as the carbon fiber was lowered in small steps, and the evoked DA transients were measured (see below) by means of FSCV. The position of the fiber was fixed when further lowering failed to increase the amplitude of the evoked DA transient.

Electrochemistry

The carbon fiber was glass-encased and a seal was produced by heating the glass capillary with a pipet puller (PUL-1, WPI, Sarasota, FL). A wire covered with silver paint was inserted in the capillary to make contact with the carbon fiber and secured with shrink tubing coated with epoxy. The exposed portion of the fiber was cut to a length of 100-150 uM.

All carbon-fiber electrodes were pre-calibrated in an electrochemical cell connected to a 6-port pressure injection valve (Upchurch Scientific, Oak Harbor, WA). Electrodes were cleaned prior to calibration with 2-propanol containing activated carbon. Artificial cerebrospinal fluid (aCSF; 145 mM Na^{+} , 2.7 mM K^{+} , 1.22 mM Ca^{2+} , 1.0 mM Mg^{2+} , 150mM Cl^{-}, 0.2mM ascorbate, 2mM $Na^{2}HPO^{4}$, pH 7.4±.05) was passed through the electrochemical cell using a pump (Multi-Phaser, YA-12, Yale Apparatus, Holliston, MA). The loop injector was loaded with DA standards at concentrations of 100nM, 200nM, 500nM, and 1000nM. DA was dissolved in ASCF. Only electrodes with linear responses to standards of increasing concentration were kept for the *in vivo* voltammetric measurements.

Background-subtracted cyclic voltammograms were generated at 10 Hz by applying a 8.5 ms triangular waveform that ramped from -0.4 V to +1.3V and back to -0.4 V at a scan rate of 400 V/s. The potential was held at -0.4 V between each scan to promote cation absorption at the surface of the carbon fiber. All potentials were measured with respect to the Ag/AgCl reference electrode. The waveform was generated using LabVIEW (National Instruments, Austin, TX) and a multifunction data acquisition board (PCI-6052E, National Instruments, Austin, TX).

A PCI-6711E (National Instruments, Austin, TX) board was used to perform waveform acquisition, and data collection. A synchronization signal from the PCI-6711E board was sent to the external input of a multi-channel pulse generator (Master-8, A.M.P.I, Israel) and used to trigger the electrical stimulation 5 s after the start of each recording. The stimulation was patterned so as to prevent overlap with the voltammetric scans. This was accomplished by confining pulse generation to the 91.5 ms intervals

separating the triangle waves. Voltages generated by the Master-8 were converted to constant currents via a stimulus isolation unit (AM-2200, AM-Systems, Carlsborg, WA). The carbon-fiber electrode was secured to a stereotaxic arm and attached to the headstage amplifier.

Recording and quantification of DA transients

The position of the carbon fiber was adjusted until voltammograms were obtained with a reliable cyclic voltammetry signature characteristic of DA, with a peak oxidation at roughly 0.6 V and a reduction peak at -0.2 V. Thereafter, the smallest current necessary for DA detection was evaluated on the basis of voltammograms with a signal to noise ratio (S/N) superior to 3 as measured by the Tarheel CV © software. Using this threshold current as a starting point, an ascending sweep of currents was constructed by selecting values spaced 0.1 or 0.2 apart in increments of $\log_{10}$ unit. Six recordings were acquired at each current. This procedure was carried out for two experimental conditions, one for electrical stimulations with a pulse duration of 0.1 ms, and one for electrical stimulations with a pulse duration of 2 ms. Lower stimulation currents and pulse durations are typically employed in ICSS experiments whereas FSCV more commonly uses higher stimulation parameters. By including pulse durations of 0.1 ms and 2 ms, and stimulating over a wide range of currents, the data can help bridge the results obtained in these two types of experiments.

Two different carbon-fiber electrodes were used to record from both hemispheres because lowering the same carbon-fiber electrode twice produced too much damage.

Peak detection to quantify DA transients was performed using a customized routine in MATLAB (The Mathworks, Natick, MA). The maximal change in peak oxidation currents was measured during the rising phase of the triangle wave. For conversion into molar concentrations, these peak currents were then compared to *in vitro* post-calibration measurements. If the electrode was damaged upon removal at the end of the experiment, pre-calibration recordings were used instead. A mean and standard error of the mean were computed for each current. Traces that represent changes in peak oxidation current as a function of time were plotted as a function of time at the potential on the triangle wave that corresponds to the peak concentration of DA. A mean and standard error of the mean were computed at all time points for each current.

Histology

After the completion of the experiment, a lethal dose of sodium pentobarbital (120 mg/rat) was administered. A stimulating electrode was lowered to the sites at which the voltammetric recordings were obtained, and a 1 mA anodal current was applied for 15 s to deposit iron ions at these locations. A 1 mA anodal current was also passed through the MFB stimulating electrode. The animals were then perfused intracardially with 0.9% sodium chloride, followed by a formalin- Prussian Blue solution (10% formalin, 3% potassium ferricyanide, 3% potassium ferrocyanide, and 0.5% trichloroacetic acid) that forms a blue reaction with the iron deposited at the tip of the electrode. Then, the brains were removed and fixed with 10% formalin solution. Sagittal sections, 40 µm thick, were cut with a cryostat (Thermo Scientific) and examined to confirm placements of the carbon fibers in the NAc shell and the stimulating electrode in the MFB.

RESULTS

Histology

The tips of the stimulation electrodes were localized within plates 56-60 of the Paxinos and Watson atlas, -2.7 to -3.2 mm posterior to Bregma (see Figure 4B). The position of the carbon fibers was mostly in the medial NAc shell with the exception of one found in the middle of the core (see Figure 4A). Sections were within plates 20-29, 0.5 to 2.0 mm anterior to Bregma.

Behaviour

Time allocation, expressed as the proportion of trial time the animal worked for the electrical stimulation, was measured to assess the rewarding efficacy of the MFB electrodes. The vigorous operant performance observed ensures that the stimulation that drove the recorded DA transients was, in fact, rewarding. The electrode was assumed to produce a potent reward if a range of frequencies could be found to produce maximal time allocation. For all animals included in the study, a sigmoidal curve relating time allocation to stimulation frequency was obtained (Figure 5). The currents required to obtain near-maximal time allocation at the higher frequencies ranged between 230 and 590 μA.

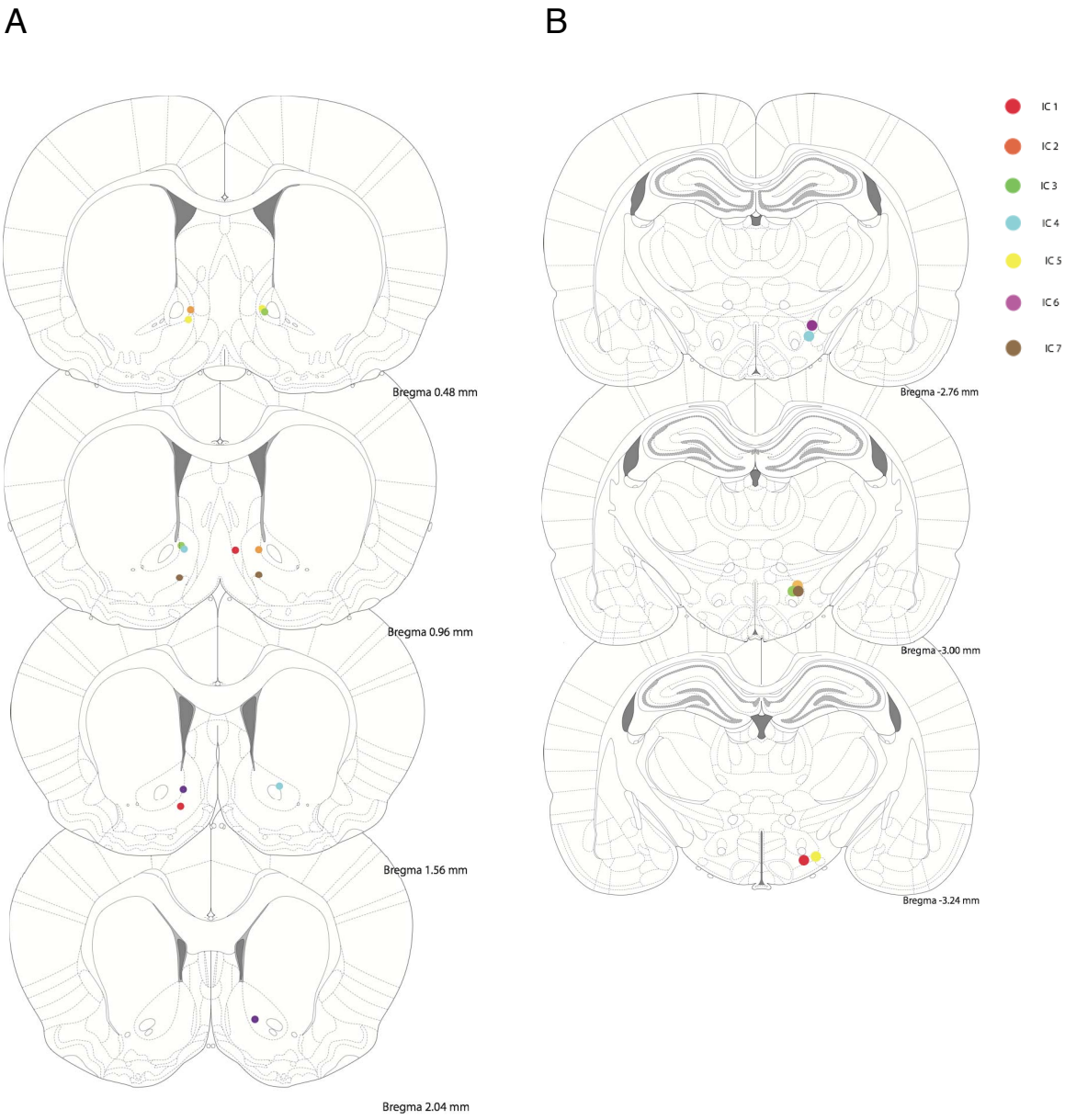

Figure 4. Location of the tips of A) the recording carbon fibers and B) the stimulating electrodes.

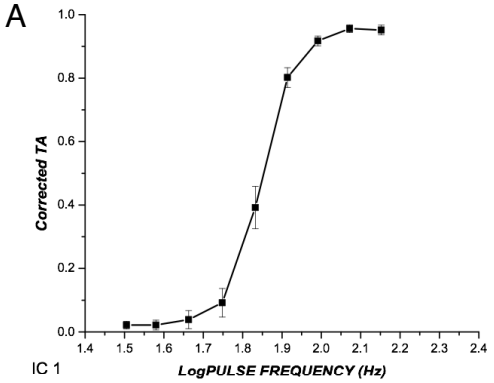
A
Corrected TA
LogPULSE FREQUENCY (Hz)
IC 1

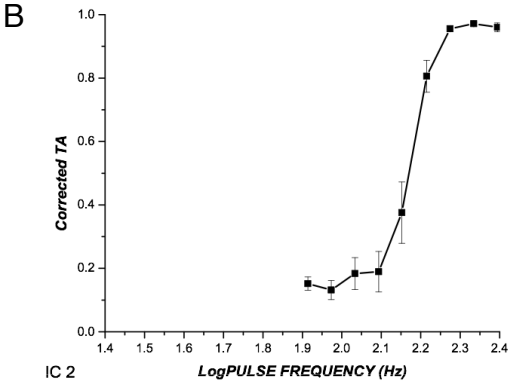
B
Corrected TA
LogPULSE FREQUENCY (Hz)
IC 2

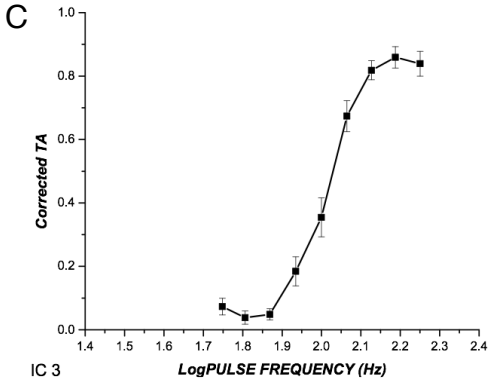
C
Corrected TA
LogPULSE FREQUENCY (Hz)
IC 3

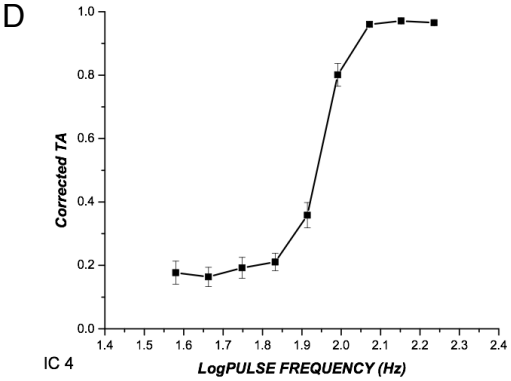
D
Corrected TA
LogPULSE FREQUENCY (Hz)
IC 4

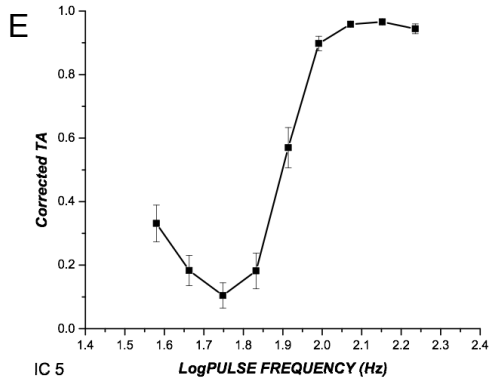
E
Corrected TA
LogPULSE FREQUENCY (Hz)
IC 5

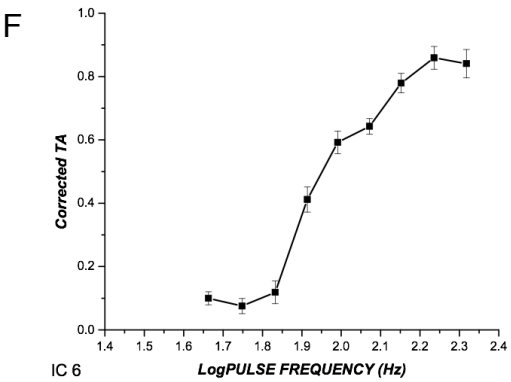
F
Corrected TA
LogPULSE FREQUENCY (Hz)
IC 6

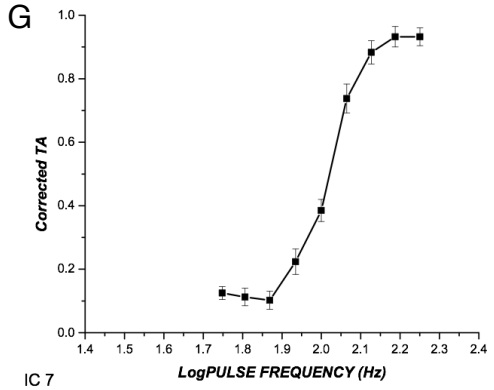
G
Corrected TA
LogPULSE FREQUENCY (Hz)
IC 7

Figure 5. Behavioural screening. All rats included in the study, displayed a sigmoidal curve relating time allocation (panels A-G), expressed as the proportion of trial time the animal worked for the electrical stimulation, to the pulse frequency. Error bars represent 95 % confidence intervals. The stimulation currents were A) 590 µA, B) 230 µA, C) 380 µA, D) 230 µA, E) 300 µA, F) 380 µA and G) 300 µA.

Neurochemical response to MFB stimulation

All DA transients were time-locked to the stimulation trains and all voltammograms had a signature characteristic of DA, with a peak oxidation at roughly 0.6 V and a reduction peak at -0.2 V. The quality of the signature was comparable for both hemispheres (see Figure 6 and 7). In most cases, changes in DA levels lasted between 2 to 3 s. Together, these observations indicate that recording sites were located in the vicinity of DA terminals and that all electrodes recorded clear voltammetric signals successfully in both hemispheres.

DA transients were observed in both the ipsi- and contralateral hemispheres during MFB stimulation in all rats (Figure 8). In 3 of the 7 rats, the maximal amplitude of the DA transients observed was larger in the ipsi- compared to the contralateral side by roughly 5, 2.7 or 2.3 times. In the four remaining rats, the maximal amplitude was the same across hemispheres for both pulse durations.

The dependence of the DA transients on current and pulse duration was examined in both hemispheres. Currents necessary to obtain detectable DA transients ranged from 14 μA to 100 μA at a pulse duration of 2 ms, and 112 μA to 891 μA at a pulse duration of 0.1 ms. The $\text{ratio}_{\text{contra/ipsi}}$ for threshold currents for each rat, at each pulse duration, was comparable, hovering around 1 in most cases (pulse duration of 2 ms, M = 1.30, SEM = 0.26; pulse duration of 0.1 ms, M = 1.01, SEM = 0.19) (see Figure 9). The correlation

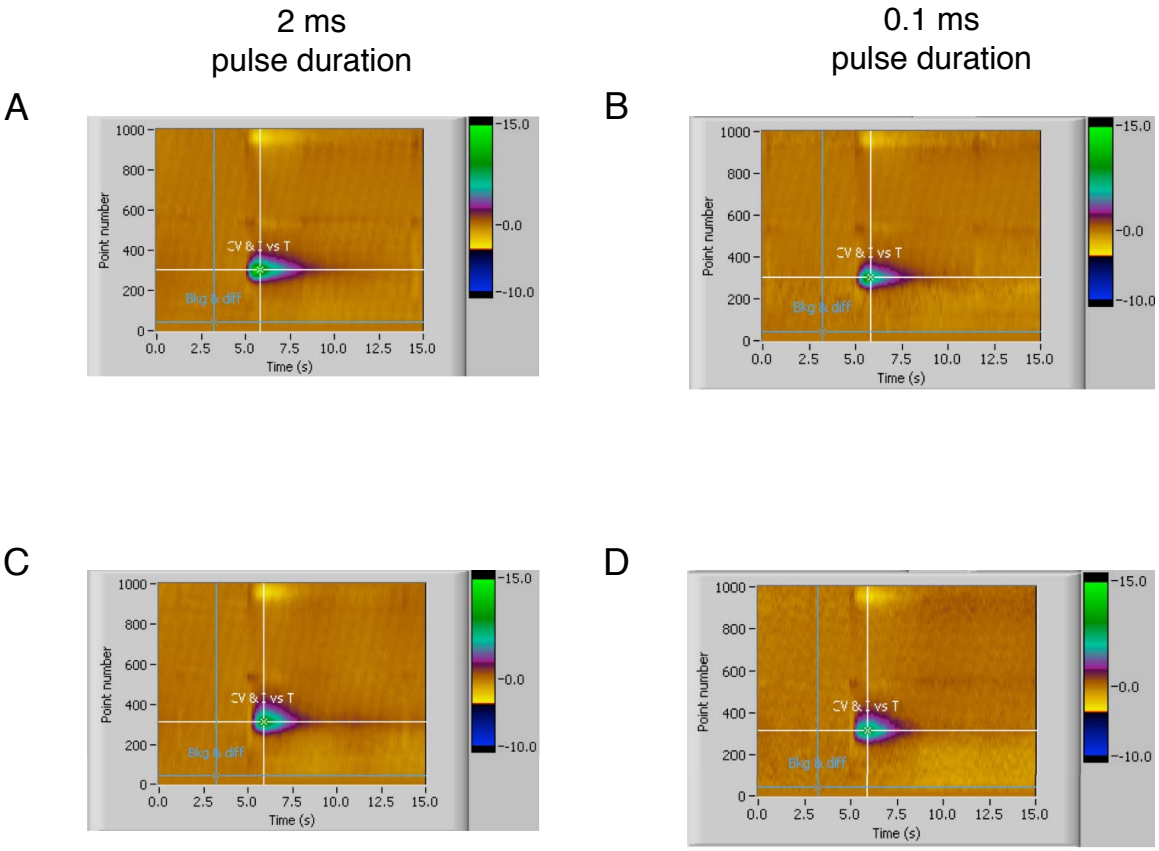

Figure 6. Voltammograms from IC 1. These color plots contain 150 background-subtracted cyclic voltammograms acquired over 15 s. The changes in voltammetric current are expressed as a function of time (s) on the x axis and point number on the y axis, representing the potentials applied at the carbon fiber at each scan. These false-color voltammograms were obtained from the ipsilateral side, A and B, and from the contralateral side, C and D.

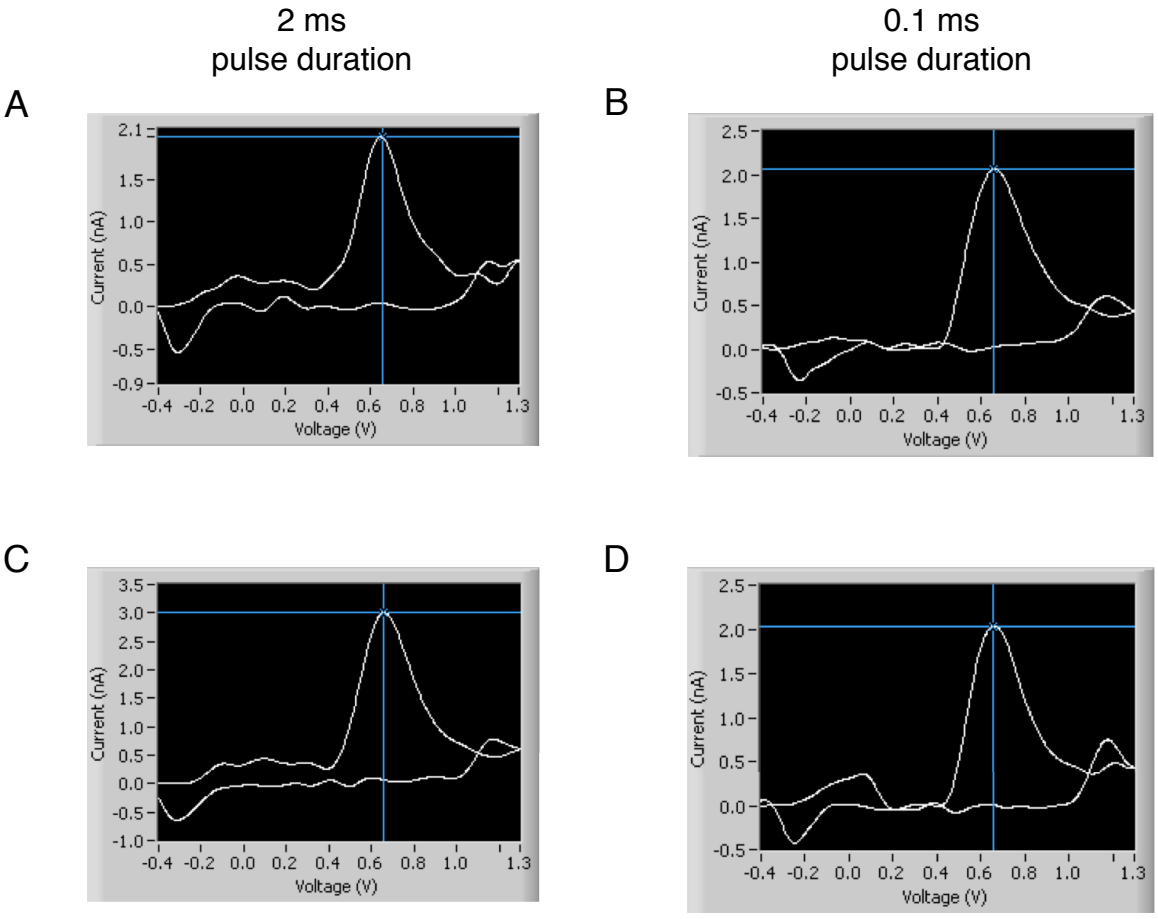

Figure 7. Cyclic voltammetry signatures from IC 1. These graphs correspond to vertical cross-sections of the false-color voltammographs such as those presented in Figure 6. These traces represent changes in voltammetric current as a function of potential applied at the carbon fiber for the point in time when DA concentration was maximal. A peak oxidation is observed at roughly 0.6 V and a reduction peak at -0.2 V. The signatures were comparable at threshold currents for the ipsilateral side, A and B, and for the contralateral side, C and D.

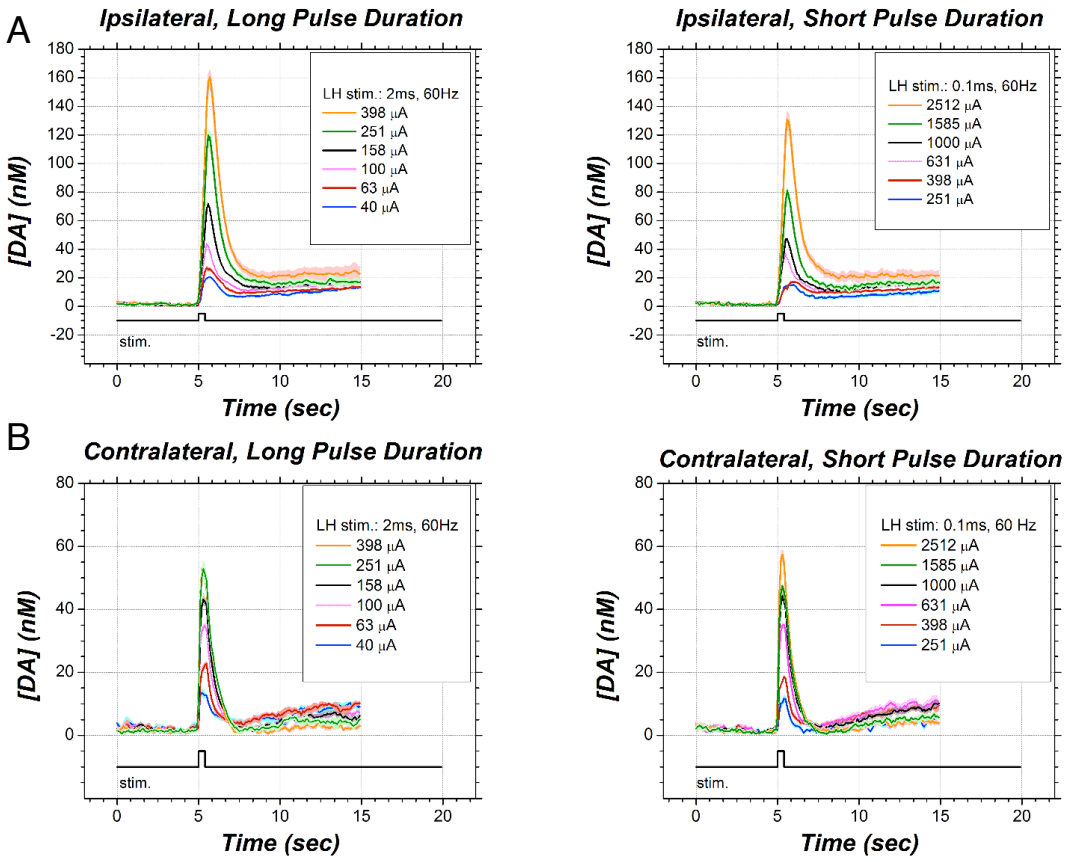

Figure 8. DA transients in response to current sweeps. Representative voltammetric measurements, for rat IC 1, showing DA changes as a function of time in the NAc shell A) ipsilateral to the MFB stimulation and B) contralateral to the MFB stimulation. These graphs correspond to horizontal cross-sections of the false-color voltammograms such as those presented in Figure 5. These traces represent voltammetric changes as a function of time for the potential at which DA concentration was maximal. The stimulation pulse frequency was fixed at 60 Hz with a train duration of 500 ms. The long pulse duration was 2 ms, and the short pulse duration 0.1 ms. The stimulation was delivered 5 s after the onset of each voltammetric recording.

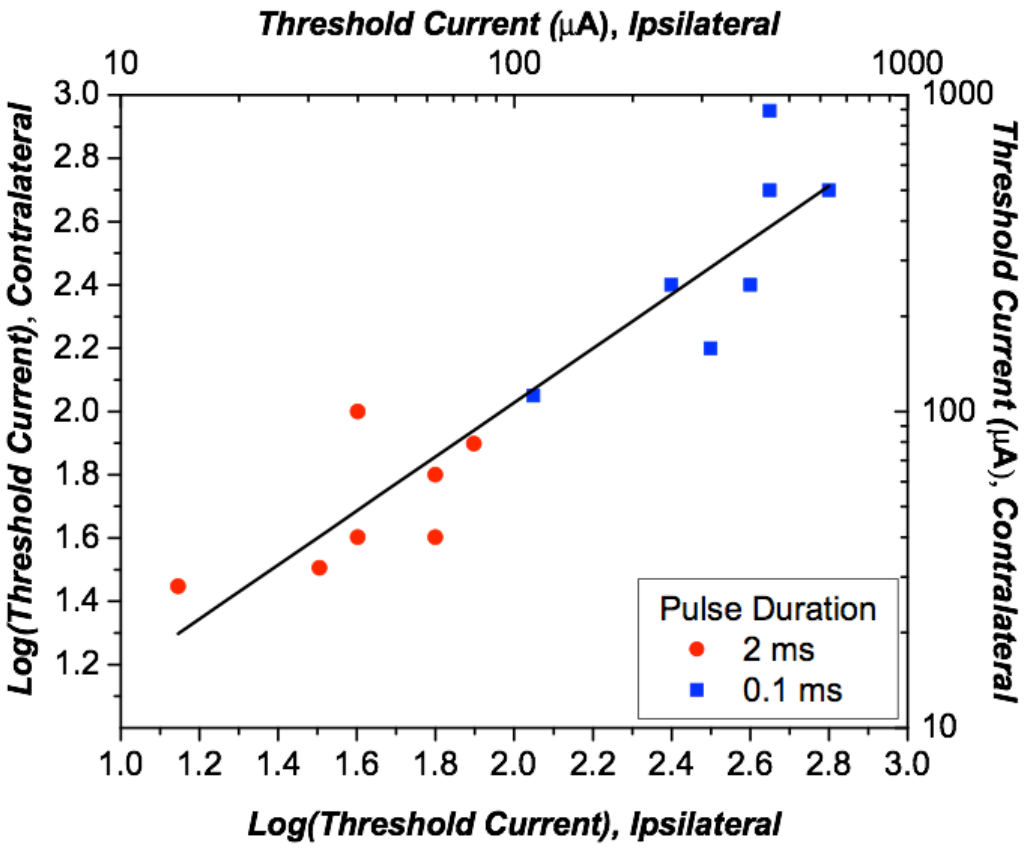

Figure 9. Threshold currents at both pulse durations. The red circles are for the threshold currents for MFB stimulation with a pulse duration of 2 ms, and the blue squares for a pulse duration of 0.1 ms. The Pearson correlation coefficient is r(26) = .93.

between threshold currents recorded in the ipsilateral NAc and the threshold currents recorded in the contralateral NAc was high ($r(26) = 0.93$).

The growth in the amplitude of DA transients was linear ($r^2 = [0.75, 0.99]$, with the exception of one animal in one hemisphere) (see Figure 10). The poorer linear fits corresponded to cases where the largest currents failed to further increase the magnitude of DA transients and could be due to damage during the lowering of the recording electrode in the NAc that presumably reduced its sensitivity to higher DA concentrations.

The amplitude of the DA transients grew more steeply as a function of current in the ipsilateral than in the contralateral hemisphere (pulse duration of 2 ms, $M_w = .41$, $t_w(4) = 3.11$, $p = .02$; pulse duration of 0.1 ms, $M_w = .31$, $t_w(4) = 4.09$, $p = .01$, statistics were computed following a 1-time winsorization (Tukey & McLaughlin, 1963); this effect was seen in 6 of the 7 rats. The $ratios_{contra/ipsi}$ for the slope representing DA growth were higher than 1, ranging from 1.18 to 3.23 for DA transients recorded at 2 ms pulse duration ($M = 1.91$, $SEM = 0.30$) and from 1.19 to 2.11 for DA transients recorded at 0.1 ms pulse duration ($M = 1.47$, $SEM = 0.18$), with the exception of one animal (pulse duration of 2 ms, $ratio_{contra/ipsi} = 0.83$; pulse duration of 0.1 ms, $ratio_{contra/ipsi} = 0.61$) (see Figure 10 and Table 1).

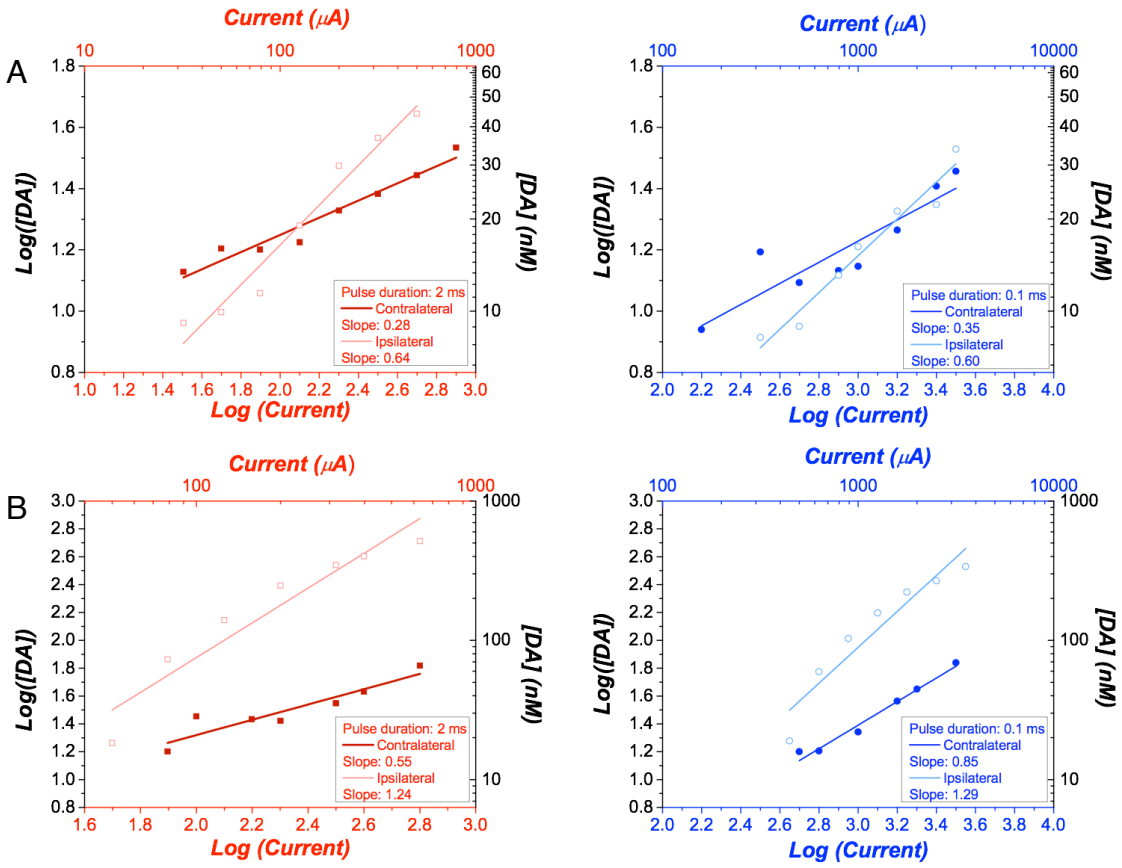

Figure 10. Growth in DA transients as a function of current. Representative graphs for rats IC 6 (row A) and IC 7 (row B) showing peak DA concentrations. The pale lines represent linear fits for voltammetric measurements obtained ipsilateral to the MFB stimulation, and the dark lines represent the fits for measurements contralateral to the MFB stimulation. The stimulation pulse frequency was fixed at 60 Hz with a train duration of 500 ms. The long pulse duration was 2 ms, and the short pulse duration 0.1 ms.

DISCUSSION

Detection of bilateral DA transients

This study corroborates earlier findings suggesting that part of the substrate recruited by MFB stimulation includes descending, non-DA neurons (Shizgal, et al., 1980; Biejalew & Shizgal, 1982, Biejalew & Shizgal, 1986). DA transients were observed in the hemisphere opposite to the MFB stimulation site in all rats. Since midbrain DA projections are overwhelmingly unilateral (Lindvall & Björklund, 1974; Swanson, 1982; Ikemoto, 2007), DA transients evoked by contralateral MFB stimulation must entail direct activation of non-DA neurons that directly or indirectly relay excitation to the contralateral VTA. Anatomical studies suggest a disynaptic route (Satoh & Fibiger, 1986; Oakman et al., 1995).

Current thresholds for DA transients

Trans-synaptic activation of the DA fibers is presumably the only mechanism for significant DA activation in the contralateral NAc. Based on the higher excitability of non-DA compared to DA fibers (Yeomans, 1989), this mechanism should also be the main source of DA activation in the ipsilateral NAc at lower currents. Threshold currents were comparable on both sides of the brain at both pulse durations. This result not only suggests that indirect DA activation is the only neural mechanism driving DA transients in the ventral striatum, at threshold currents, even in the ipsilateral NAc, but also that this activation is sustained by the same type of DA activation and, possibly by the same subpopulation of neurons in both hemispheres. The correlation between threshold

currents recorded in the ipsilateral NAc and the threshold currents recorded in the contralateral NAc was high, consistent with the notion that a common substrate is involved. Consequently, disynaptic DA activation might be equally important in producing transient changes in DA release in both hemispheres at near threshold currents.

Growth of DA transients

The growth in the amplitude of DA transients in response to increasing currents was expected to be steeper in the ipsilateral NAc based on the three proposed sources of DA activation for this hemisphere: direct, monosynpatic and disynaptic. This is in contrast to the sole source of DA activation proposed for the contralateral hemisphere, a disynaptic activation. Consistent with this prediction, the growth in the amplitude of DA transients was steeper in the ipsilateral side for 6 of the 7 rats. This result highlights the importance in considering all the possible routes of DA activation when trying to identify the neural network underlying the phenomenon of ICSS.

These findings point to a major role for indirect DA activation in producing transient changes in DA, a role more substantial than previously acknowledged. In fact, it is often believed that, MFB stimulation can be used to study the effect of directly activating the VTA-NAc pathway (Suaud-Chagny, Chergui, Msghines & Gonon, 1995; Yavich, 2000; Pillola, Melis, Perra, Muntoni, Gessa & Pistis, 2007; Yavich & Tanila, 2007). However, we demonstrate that, at pulse durations and currents that are typically used in ICSS and FSCV experiments, untangling the contribution of directly versus indirectly activating midbrain DA neurons is not a simple matter, due to the multiple routes by which excitation elicited by MFB stimulation may reach VTA DA neurons.

Thus, it becomes crucial to further investigate the implication of the indirect DA activation during MFB stimulation insofar as the electrical stimulation of this brain region is used as a tool to probe mesolimbic DA pathways in both ICSS and FSCV experiments.

Identifying neural components of trans-synaptic DA activation

Many different neural pathways course through the MFB (Nieuwenhuys et al., 1982; Veening et al., 1982) (see Figure 2), many of which are potentially implicated in activating midbrain DA neurons. There are three possible types of excitation including a direct, monosynaptic and disynaptic DA activation (Satoh & Fibiger, 1986; Steinenger, et al., 1992; Oakman, et al., 1995; Geisler, et al., 2007) (see Figure 3).

Other than the direct activation of the ascending DA axons as a mechanism to produce DA transients in the NAc (see Figure 3a), functional (Chergui, et al., 1993; Overton & Clark, 1992; You, Chen & Wise, 2001; Grace, et al., 2007; Sombers, et al., 2009) and ICSS studies (Herberg & Rose, 1990; Sombers, et al., 2009) point to the importance of glutamate afferents to the VTA as a source of phasic activity in midbrain DA neurons. Anatomical experiments reported glutamate projections that could activate DA cell bodies either monosynaptically or disynaptically, via the LDTg/PPTg, (Satoh & Fibiger, 1986; Steinenger et al., 1992; Semba & Fibiger, 1992; Geisler, et al., 2007). These glutamate afferents could originate from the mPFC, the LPOA, the VP, the SLEA and the LH (see Figure 3b and 3c).

Based on functional (Forster & Blaha, 2000; Blaha & Phillips, 1996; Grace, et al., 2007) and ICSS studies (Yeomans, 1985; Yeomans et al., 1997; Yeomans, et al., 2000), cholinergic neurotransmission also modulates midbrain DA activity and contributes to reward seeking. Consequently, cholinergic afferents, originating from the LDTg/PPTg and synapsing onto VTA DA neurons, may also contribute to disynaptic activation of VTA DA neurons by MFB stimulation (see Figure 3c) (Satoh & Fibiger, 1986; Steinenger, et al., 1992; Oakman, et al., 1995).

All three hypothesised routes of activation will be tested, in future experiments, for their necessity and sufficiency in producing DA transients during MFB stimulation by employing optogenetic techniques.

Optogenetics: a method of choice

The inherent heterogeneity of the MFB (Nieuwenhuys et al., 1982; Veening et al., 1982) and the lack of specificity of traditional methods used to study this pathway make the search for the identity of the neurons recruited by the MFB stimulation a challenging endeavour.

The emerging technique of optogenetics offers a promising avenue to better pinpoint the anatomy underlying ICSS. The procedure achieves unprecedented spatial and temporal control over neural activity. Through the use of viral vectors and transgenic animals, light-sensitive proteins that can function as ion channels or pumps, also called opsins, are genetically expressed in one particular subset of neurons, to be activated or inhibited by pulses of light. For instance, the protein can be expressed exclusively in cells

producing the dopamine transporter (DAT), allowing control of the activity of dopaminergic neurons. Similarly, the protein could be targeted to cells that express the choline acetyltransferase (ChAT) to alter choline neurotransmission without affecting other types of neurotransmission. In principle, opsin expression could be restricted to glutamate neurons if the viral injections were made in nuclei containing glutamatergic, but no dopaminergic somata. In addition, light pulses can be delivered and interrupted in milliseconds, a temporal scale that closely matches the scan rate of FSCV measurements, as well as the length of burst-like events such as the firing of midbrain DA neurons induced by MFB stimulation. Thus, optogenetics is a method particularly suitable for the experiments required to investigate the relative contribution of direct and indirect DA activation to DA transients recorded in terminal fields.

Silencing DA cell bodies in the VTA would provide another tool for determining unambiguously whether midbrain DA neurons can be trans-synaptically activated, either monosynaptically or disynaptically. To this end, the VTA would be transfected with enhanced halorhodopsin-3.0 (eNpR3.0), a proton pump that hyperpolarizes neurons (Gradinaru, Zhang, Ramakrishnan, et al., 2010), under the control of the DAT promotor, in the hemisphere ipsilateral to the MFB stimulation site. The light would be concurrent with the MFB stimulation. This would disrupt the putative indirect DA activation in the ipsilateral but not the contralateral DA fibers (see Figure 11a). DA transients should be reduced in the ipsilateral NAc and remain unchanged in the contralateral NAc. If the contralateral VTA was also transfected and the light was shone on that brain region, the opposite pattern should be observed. In contrast, if VTA DA neurons were excited exclusively by the direct route (i.e., via direct axonal stimulation), the optogenetic

silencing should have no effect because the stimulation site would lie downstream from the locus of silencing.

To assess whether direct DA activation produces DA transients only in the ipsilateral NAc, the same procedure as above would be repeated but channelrhodopsin-2 (ChR2), a cation channel (Boyden, Zhang, Bamberg, Nagel & Deisseroth, 2005), would be substituted for eNpR3.0. Activation of DA neurons would be triggered optically in the absence of MFB stimulation (see Figure 11b). Shining light ipsilateral to the transfected side should produce DA transients only in the ipsilateral and not the contralateral hemisphere. Moving the light to the contralateral VTA should fail to produce DA transients in either NAc. This would confirm that, as the anatomical studies have suggested, unilateral stimulation of VTA DA cell bodies does not result in transient DA release in the contralateral hemisphere.

To further investigate the monosynaptic route for activation of DA cell bodies in the VTA, gluatmatergic terminals in the VTA would be silenced optically. To this effect, eNpR3.0 could be expressed in glutamatergic neurons arising in the mPFC, LPOA, VP, SLEA or the LH, under the control of the appropriate vesicular glutamate transporter for the neural population in question (Geisler et al., 2007). The viral vectors would be

A

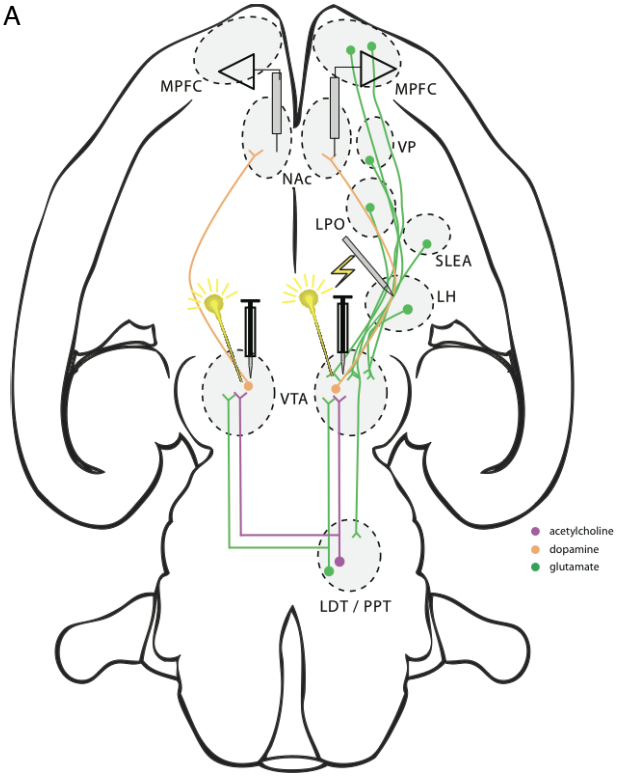
MPFC
MPFC
VP
NAc
LPO
SLEA
LH
VTA
acetylcholine
dopamine
glutamate
LDT / PPT

B

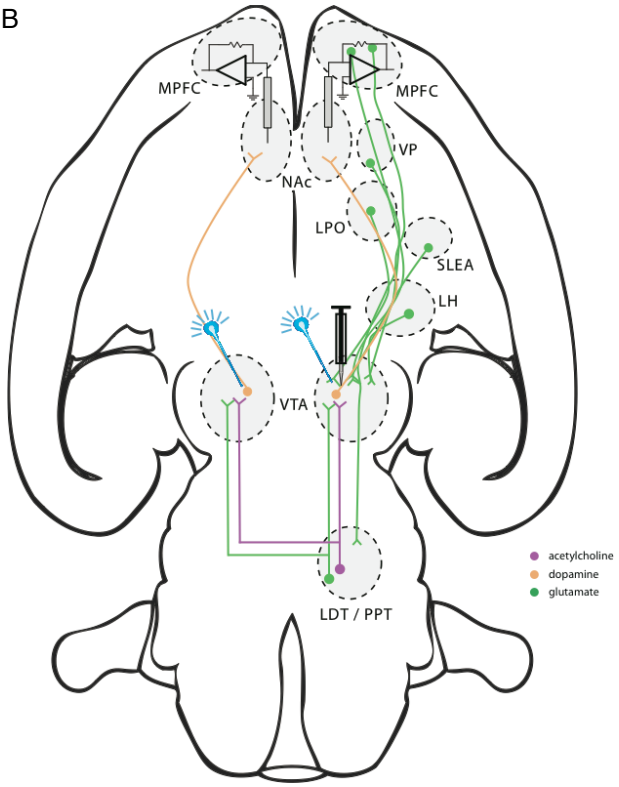
MPFC
MPFC
VP
NAc
LPO
SLEA
LH
VTA
acetylcholine
dopamine
glutamate
LDT / PPT

Figure 11. Probing the effects of specific optogenetic silencing or activation of VTA DA neurons during delivery of MFB stimulation. A) Enhanced halorhodopsin-3.0 would be expressed under the control of the DAT promotor, in the VTA ipsilateral to the MFB stimulation site. The light would be shone concurrently with the delivery of MFB stimulation. A reduction in DA transients is expected in the ipsi- but not the contralateral NAc. If VTA DA neurons were excited exclusively by the direct route (e.g., via direct axonal stimulation), the optogenetic silencing should have no effect. B) Channelrhodopsin-2 would be expressed under the control of the DAT promotor unilaterally. Shining light ipsilateral to the transfection site should produce DA transients only in the ipsilateral and not the contralateral hemisphere. Figure prepared by Ivan Trujillo and Peter Shizgal (personal communication).

injected into these nuclei in the same hemisphere as the stimulation electrode. The different brain regions would be targeted one at the time, all in separate animals. Sufficient time would be provided for opsin transport to the VTA terminals of the glutamatergic neurons (as confirmed by double immunofluorescence). Light would then be applied to the VTA ipsilateral to the MFB stimulation electrode during delivery of stimulation trains (see Figure 12a). On the basis of the foregoing discussion, this manipulation would be expected to block monosynaptic activation of VTA DA neurons and reduce DA transients in the ipsilateral but not the contralateral NAc. If DA transients were also attenuated in the contralateral NAc, this would suggest that there is a significant contingent of glutamate fibers arising from forebrain nuclei that decussate between the MFB stimulation site and the VTA. If this is the case, shining light in the contralateral VTA should reduce contralateral DA transients and leave ipsilateral DA transients intact.

To corroborate these conclusions, the same procedure would be repeated, but substituting ChR2 for eNpHR3.0. Light would be applied to excite glutamate terminals in VTA ipsilateral to the transfection site (see Figure 12b). If glutamatergic excitation is sufficient to monosynaptically activate midbrain DA neurons, DA transients should be observed in the ipsilateral but not the contralateral NAc. Shining light in the contralateral VTA should fail to produce DA transients in either hemisphere unless the descending glutamatergic projection decussate en route to the contralateral VTA.

Both of the experiments probing the contribution of descending glutamate

A

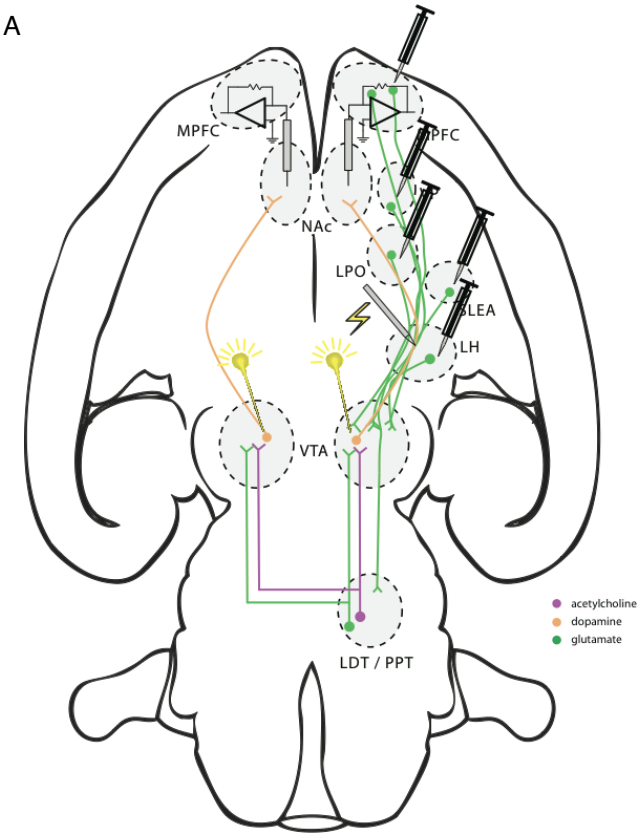
MPFC
NAc
LPO
LH
VTA
LDT / PPT
acetylcholine
dopamine
glutamate

B

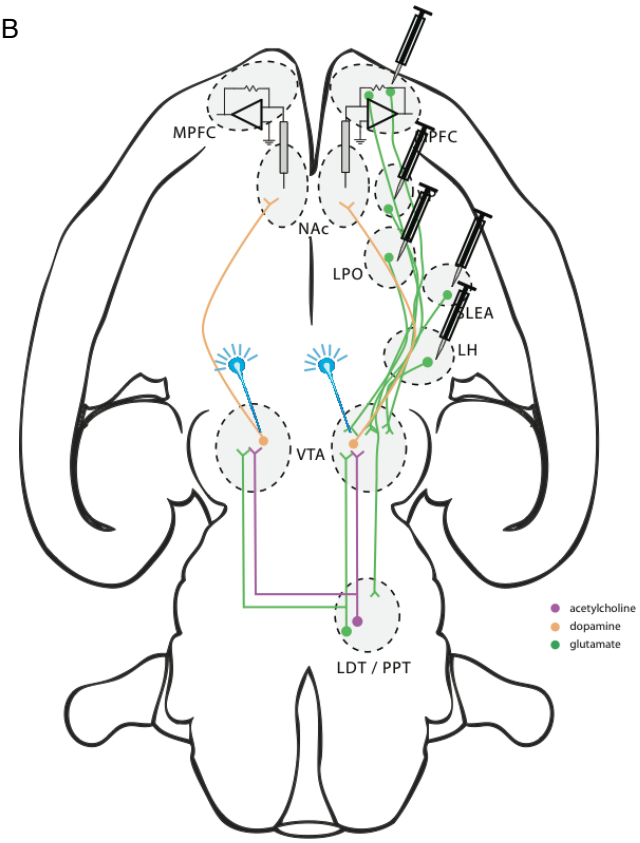
MPFC
NAc
LPO
LH
VTA
LDT / PPT
acetylcholine
dopamine
glutamate

Figure 12. Probing the effects of specific optogenetic silencing or activation of VTA glutamatergic terminals during delivery of MFB stimulation. A) Enhanced halorhodopsin-3.0 would be expressed in glutamatergic neurons arising in the mPFC, LPOA, VP, SLEA or the LH, under the control of the appropriate vesicular glutamate transporter for the neural population in question. The viral vectors would be injected into these nuclei in the same hemisphere as the stimulation electrode. The light would be shone concurrently with the delivery of MFB stimulation. A reduction in DA transients is expected in the ipsilateral but not the contralateral NAc. B) Channelrhodopsin-2 would be expressed unilaterally in the same glutamate neurons and under the control of the same promotors as in A). Light shone in the VTA ipsilateral to the transfection site is expected to produce DA transients in the ipsi- but not contralateral NAc. Shining light in the contralateral VTA should fail to produce DA transients unless the descending glutamatergic projection decussate en route to the contralateral VTA. Figure prepared by Ivan Trujillo and Peter Shizgal (personal communication).

projections to the VTA to DA activation would also determine which of the multiple groups of forebrain glutamate cell bodies that project through the MFB contribute to the recruitment of VTA DA neurons by MFB stimulation.

To identify the second subpopulation of neurons in the chain responsible for disynaptic DA activation, the glutamatergic and cholinergic VTA terminals of LDTg/PPTg neurons would be silenced selectively by optical means. eNpR3.0 would be expressed in LDTg/PPTg neurons, under the control of ChAT or VGLUT2 promotors, in the hemisphere ipsilateral to the MFB stimulation electrode. Sufficient time would be provided for opsin transport to the VTA terminals (as confirmed by double immunofluorescence). Light applied to the VTA ipsilateral to the MFB stimulation electrode during delivery of stimulation trains (see Figure 13a) should disrupt the putative glutamatergic or cholinergic link in the disynaptic circuit exclusively on the ipsilateral side, reducing DA transients in the ipsi- but not contralateral NAc. In contrast, moving the optical inhibition to the contralateral VTA should reduce DA transient in the contra- but not ipsilateral NAc.

Employing the same preparation but substituting ChR2 for eNpHR3.0, the activation of glutamatergic or acetylcholine terminals in the VTA is expected to be sufficient to produce DA transients in the ipsi- but not the contralateral NAc in response to the optical stimulation, unless the optical stimulation produces antidromic activation of the cell bodies in the LDTg/PPTg (see Figure 13b).

These experiments would serve as a foundation for later studies that would combine behavioural and optogenetic methods to identify components of the neural

A

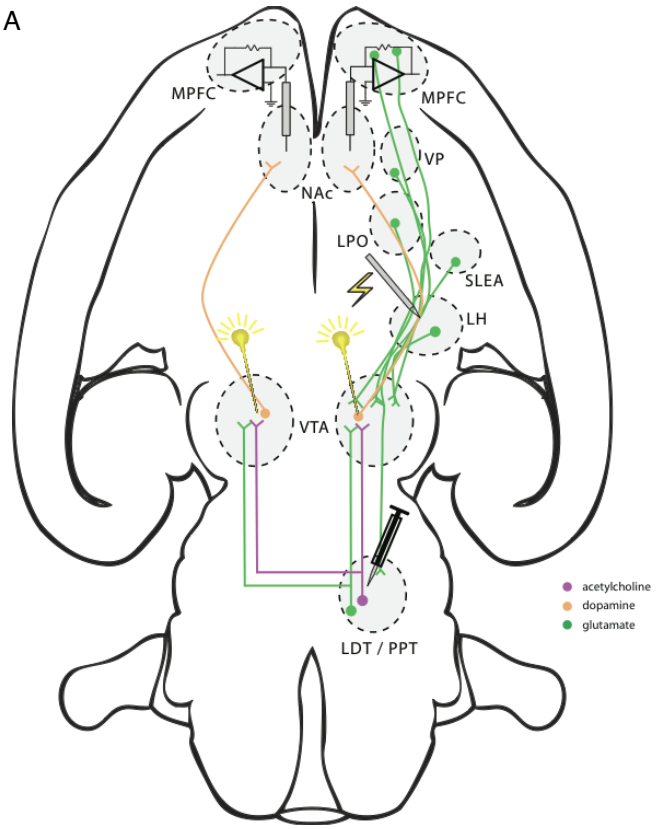
MPFC
MPFC
VP
NAc
LPO
SLEA
LH
VTA
LDT / PPT
acetylcholine
dopamine
glutamate

B

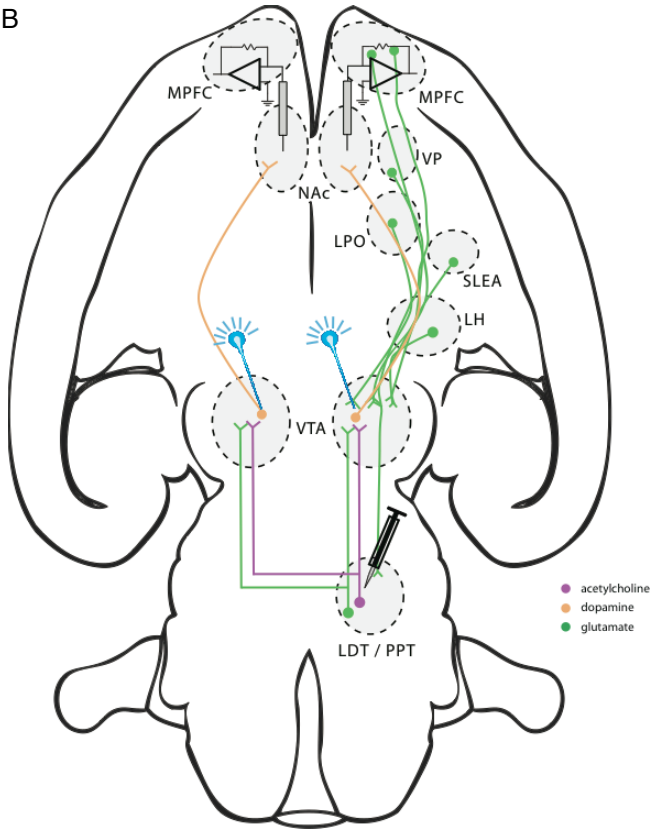
MPFC
MPFC
VP
NAc
LPO
SLEA
LH
VTA
LDT / PPT
acetylcholine
dopamine
glutamate

Figure 13. Probing the effects of specific optogenetic silencing or activation of VTA glutamatergic and cholinergic terminals originating from LDTg/PPTg neurons during delivery of MFB stimulation. A) Enhanced halorhodopsin-3.0 would be expressed in LDTg/PPTg neurons, under the control of promotors for ChAT or vesicular glutamate transporter 2 (VGLUT2), in the hemisphere ipsilateral to the MFB stimulation electrode. The light would be shone concurrently with the delivery of MFB stimulation. A reduction in DA transients is expected in the ipsi- but not contralateral NAc. In contrast, moving the optical inhibition to the contralateral VTA should reduce DA transient in the contra- but not ipsilateral NAc. B) Channelrhodopsin-2 would be expressed unilaterally in the same neurons and under the control of same promotors as in A). Light shone in the VTA ipsilateral to the transfection site is expected to produce DA transients in the ipsi- but not contralateral NAc, unless the optical stimulation produces antidromic activation of the cell bodies in the LDTg/PPTg. In contrast, moving the optical stimulation to the contralateral VTA should produce DA transient in the contra- but not ipsilateral NAc. Figure prepared by Ivan Trujillo and Peter Shizgal (personal communication).

substrate for the rewarding effect of MFB stimulation.

EXPERIMENT 2

INTRODUCTION

An overarching goal driving the current investigation is to tie specific valuation stages involved in ICSS (e.g., integration of reward strength) to transient changes in DA release in the mesolimbic system. In doing so, the ideal approach would include characterisation of time allocated to MFB ICSS with simultaneous neurochemical detection of DA transients in the NAc using fast-scan cyclic voltammetry. Experiment 2 served as a preparatory phase for such work. Behavioural data were acquired separately, followed by voltammetry measurements obtained under anaesthesia.

Moisan and Rompré (1998) proposed that midbrain DA neurons are involved in an early stage of reward valuation of ICSS in the posterior mesencephalon, integrating the post-synaptic effects of impulse flow produced by the rewarding stimulation. It has been demonstrated that the neural circuit subserving this spatio-temporal integration process acts as a monotonic counter of the total number of action potentials triggered by the stimulation (Gallistel, 1978; Simmons & Gallistel, 1994; Gallistel, et al., 1981). Implied is that the output of the spatio-temporal integration process is independent of the means by which the aggregate firing rate is achieved; a given aggregate firing rate will have the same effect, regardless of whether it arises from many neurons firing at low frequency or fewer neurons firing at a higher frequency.

Moisan and Rompré (1998) stimulated the posterior mesencephalon and recorded

activity of DA cell bodies in the VTA. They found that combinations of stimulation currents and pulse frequencies that supported the same level of ICSS also produced equivalent rates of firing in the DA neurons. From these results, Moisan and Rompré (1998) concluded that DA neurons could be responsible for integrating the aggregate firing rate triggered in the neurons directly activated at the tip of the stimulating electrode. Alternatively, they also hypothesised that DA neurons could be a downstream series element in the reward circuitry, relaying the integrated reward signal to efferent stages of the neural circuitry. If so, changes in DA release should be related monotonically to aggregate impulse flow in the directly stimulated neurons (Gallistel et al., 1981). The way the parameters of the stimulation train interact has been estimated from behavioural trade-off experiments. The relationships established by such experiments provide criteria for judging whether the responses of dopamine neurons can or cannot track the aggregate impulse flow induced by the stimulation and the post-synaptic integration of this signal. To estimate the difference in aggregate firing rate between combinations of stimulation parameters frequency trade-off experiments are often conducted.

Trade-off experiments find combinations of two stimulation parameters that produce equivalent behavioural performance. The monotonicity of the relationship between aggregate impulse flow and performance implies the monotonicity of all stages of the neural circuitry that intervene between the stimulation electrode and the observed behavioural response (Gallistel et al., 1981). The pulse frequency determines the number of action potentials triggered by the stimulation per unit of time, whereas the current determines the spatial extent of the region of effective excitation, and thus the number of

behaviourally relevant neurons recruited by the stimulation. With the pulse frequency fixed, the current can be adjusted to produce a criterial level of behavioural performance. As the frequency is changed, the experimenter can determine the adjustments in current required. The result is a function that expresses the current required to meet the behavioural criterion as a function of the pulse frequency. Trade-off experiments conducted with animals either crossing a runway or pressing a lever to obtain electrical stimulation revealed that the relation between the reciprocal of the pulse frequency and current approximates linearity over a substantial range (Edmonds, Stellar & Gallistel, 1974; Gallistel, 1978; Gallistel & Leon, 1991a; Leon & Gallistel, 1992; Simmons & Gallistel, 1994). If so, a decrease in pulse frequency by a given amount, a halving for example, can be compensated by an increase in current by a proportional amount, for example, 2.5 times, to maintain the same level of behaviour. This relationship is called the current-frequency trade-off function. What Moisan and Rompré (1998) showed is that the firing of midbrain dopamine neurons tracks this function over a doubling range, in response to rewarding electrical stimulation of the posterior mesencephalon.

The approach of Moisan and Rompré (1998) can be pushed much further by exploring the range of pulse frequencies over which the proportionality between current and pulse frequency breaks down. Gallistel (1978) noted that the proportionality between the pulse frequency and stimulation current levels off at high pulse frequencies; beyond a certain value, further increases in pulse frequency fail to alter ICSS performance, and thus, further changes in current are no longer required to sustain a given level of behaviour. He calls this phenomenon the high-frequency roll-off, a phenomenon that likely reflects some combination of a ceiling on the maximum sustained firing frequency

of the directly stimulated axons and fatigue at downstream synaptic stages of the circuit subserving the rewarding effect. The high-frequency roll-off has been formally demonstrated to occur around 300 Hz in a subject-specific manner (Simmons & Gallistel, 1994; Solomon, Trujillo & Shizgal, 2010). It is important to note that the trade-off function levels off at the saturation point but does not inflect and begin to decline. This result implies that beyond a pulse frequency of around 300 Hz, further increases in frequency fail to alter the neural signal reflecting the post-synaptic integration of aggregate impulse flow in the directly stimulated neurons subserving the rewarding effect. If DA neurons serve as a series stage in the reward pathway, their activity must track aggregate impulse flow in the directly stimulated ICSS substrate. This requires that the activity of the DA neurons saturates at the same pulse frequency as the current-frequency trade-off function and levels off as the frequency is raised beyond this value.

Experiment 2 investigated the correspondence between the reward effectiveness of MFB stimulation, as inferred from behaviourally derived current-frequency trade-off functions, and the amplitude of DA transients in the NAc as measured by FSCV. Over the lower portion of the pulse-frequency range, DA transients increased in amplitude as the frequency was raised, in a manner consistent with behavioural data. However, the amplitude of the DA transients generally decreased over the upper portion of the pulse-frequency range, diverging from the behavioural data, which imply an increasing, but decelerating, neural response that was approaching saturation. There is no straightforward way to reconstitute the behaviourally derived trade-off function from the nucleus accumbens DA transients recorded in this study. This result casts doubt on the hypothesis

that the DA input to this terminal field constitutes an entire series stage in the neural circuit subserving self-stimulation of the MFB.

METHODS

Subjects

Subjects were 5 Long Evans male rats (Charles-River, St. Constant, QC, Canada). Animals weighed 300–350 g at their arrival. They were housed individually with ad libitum access to food and water and maintained on a 12 h light/dark reverse cycle (lights off from 08:00 to 20:00). The experimental procedures were performed in accordance with the principles outlined by the Canadian Council on Animal Care.

Intracranial Self-Stimulation

Surgery

Surgical procedures were the same as described in experiment 1. A stimulation electrode was stereotaxically aimed at the right LH level of the MFB (AP: -2.8 mm; ML: 1.7 mm; DV: 8.9 mm from the skull; all coordinates are referenced to bregma). An additional electrode was placed in the external plexiform layer of the olfactory bulb (AP: 6.2 mm; ML: -0.1 mm; DV: 5 mm from the skull; all coordinates are referenced to bregma) to serve as the anode of the stimulation circuit. Again, the location of the anode was chosen so as to place the recording site mid-way between the cathode and anode of the stimulation circuit to reduce the chance of interference between the electrical stimulation and the voltammetric measurements.

The skull above the NAc was temporarily covered with bone wax, and two

stainless steel tubes were positioned to guide the levelling of the head during the second surgery, which was performed prior to FSCV recordings.

ICSS testing

Upon recovery from surgery, shaping was conducted following the same procedure and in the same operant boxes as in experiment 1. Animals were trained to respond for 400 ms trains of 0.1 ms cathodal, constant-current pulses, delivered via a stimulation electrode aimed at the MFB. Once the rats acquired the operant response, their ICSS performance was assessed as the pulse frequency was "swept" (decremented in equal proportional intervals from trial to trial). The price of the rewarding stimulation was 4 s: the cumulative time the animal had to hold down the lever to harvest an electrical train. The dependent behavioural measure was time allocation, the proportion of trial time during which the animal worked for the electrical stimulation. Time allocation was corrected as described in Breton, et al. (2009).

Once the psychometric curves relating time allocation to pulse-frequency were stable for 5 consecutive days, current sweeps were substituted for the frequency sweeps. The current sweeps were carried out at one of the following pulse frequencies: 60, 125, 250 and 1000 Hz. The range of currents tested was selected so as to describe the sigmoidal relationship between current and time allocation. Ideally, three data points were positioned along the upper asymptote, three along the lower, and three on the rising portion. Testing was continued until stable current-sweep data were obtained for 5 consecutive days. The same procedure was then repeated for each of the 3 remaining pulse frequencies.

During the next phase of the experiment, test sessions consisted of current sweeps carried out at each of the four pulse frequencies; the order of the sweeps was randomized within session. Such test sessions were run repeatedly until stable data were obtained over five consecutive sessions.

The current-frequency trade-off function describes the changes in current required to sustain half-maximal performance as the pulse frequency is altered. This trade-off function was derived, as described below (Results), from the stable data obtained during the five final testing sessions. Upon completion of behavioural testing, voltammetric measurements were carried out.

Fast-scan cyclic voltammetry

Surgery

Surgical procedures were the same as described in experiment 1. The carbon fiber was lowered into the NAc shell (AP: 1.7 mm; ML: 1.0 mm; DV: 7 mm from the skull) and a sintered Ag/AgCl reference electrode was placed in the hemisphere contralateral to the carbon fiber.

Electrochemistry

The fabrication of the carbon-fiber electrodes, the pre-calibration methods, the FSCV measurements and the delivery of electrical stimulation were all performed as in experiment 1.

Recording and quantification of DA transients

The position of the carbon fiber was adjusted until voltammograms were obtained with a reliable cyclic voltammetric signature characteristic of DA: a peak oxidation current at roughly 0.6 V and a reduction peak at -0.2 V. DA transients were measured as the current was "swept" (incremented in equal proportion steps). Such current sweeps were acquired at pulse frequencies of 60, 130, 250 and 1000 Hz, which are the same, or nearly so, as those employed in the behavioural testing. The train duration was approximately 400 ms[1] and the pulse duration was 0.1 ms; due to the need to avoid interference with the voltammetric measurements, biphasic pulses were employed. The full ranges of currents was tested at each of the pulse frequencies.

To avoid gradual changes in the sensitivity of the carbon fiber that might affect the relative amplitude of DA transients obtained at different pulse frequencies, only one voltammogram was acquired at each given current. This ensured that a complete set of FSCV data was obtained within a short period of time.

DA quantification was performed as in experiment 1. Peak detection to quantify DA transients was performed using a customized routine in MATLAB (The Mathworks, Natick, MA). The maximal change in peak of oxidation currents was measured during the

[1] The definition of the train duration in this phase of the experiment corresponds to that employed in previous FSCV experiments (Garris, Ciolkowski, Pastore & Wightman, 1994; Kilpatric, Rooney, Michael & Wightman, 2000; Cheer, Heien, Garris, Carelli & Wightman, 2005; Beyene, Carelli & Wightman, 2010). Unfortunately, this definition differs from (and is less accurate than) the definition employed in ICSS studies, including the first phase of this experiment. In ICSS studies, the train duration is defined as the interval between the leading edges of the first and last pulses in the train. Thus, the number of pulses in the train is one greater than the number of periods (the interval separating the leading edges of two consecutive pulses). In the FSCV experiments, the last pulse required to instantiate this definition has been omitted. This causes the train duration, as defined in the ICSS studies, to be one period shorter than the specified value and to vary modestly as a function of pulse frequency.

rising phase of the triangle wave. For conversion into molar concentrations, these peaks currents were then compared to *in vitro* post-calibration measurements.

Histology

The procedure to confirm the location of the tips of the MFB stimulating electrodes was the same as in experiment 1.

RESULTS

Histology

The tips of the stimulation electrodes were localized within plate 169 of the Paxinos and Watson atlas, 1.9 mm lateral to the midline (see Figure 14). There was little variation in electrode placement, which suggests that there was little corresponding variability in the neural substrate recruited by the stimulation electrodes.

Psychophysical functions

The four psychometric curves relating time allocation to the common logarithm of the current are plotted, for each rat, in the left-hand panels of Figure 15; each curve was obtained at a different pulse frequency (60, 125, 250 or 1000 Hz). All curves are roughy sigmoidal in form, and they are displaced systematically leftward by increases in the pulse frequency. The trade-off functions in the right-hand panels of Figure 15 describe the horizontal spacing of the psychometric curves in the left-hand panels. The dashed horizontal line represents the criterion used to derive the trade-off functions, which lies at the mid-point between the maximal and minimal time allocation observed over the entire set of four psychometric curves. Thus, the trade-off functions express the current required to sustain half-maximal time allocation (referred to hereafter as the "required current") as a function of the pulse frequency.

In all 5 rats, the required current decreased monotonically as the pulse frequency was increased from 60 to 1000 Hz, and the slope of the trade-off function in the double

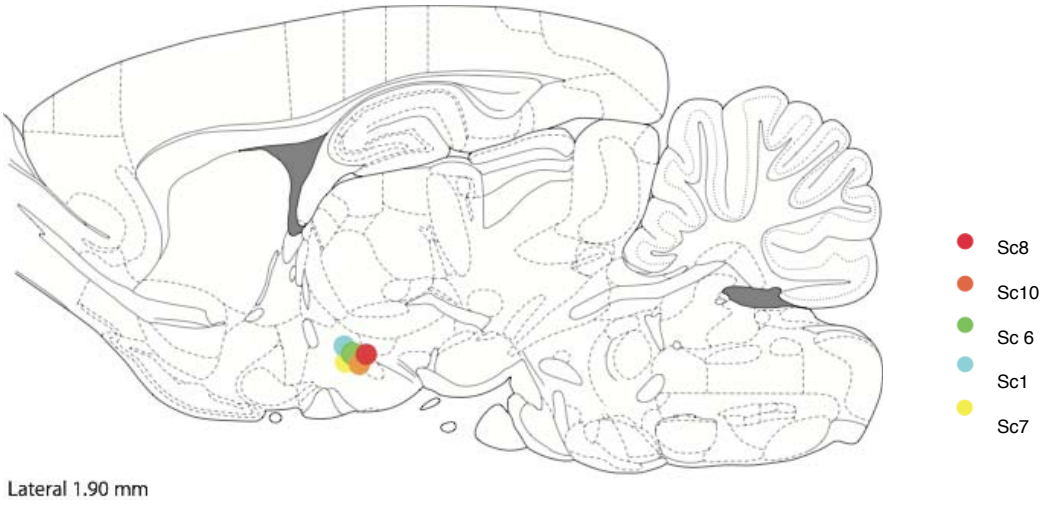

Figure 14. Location of the tips of the stimulating electrodes.

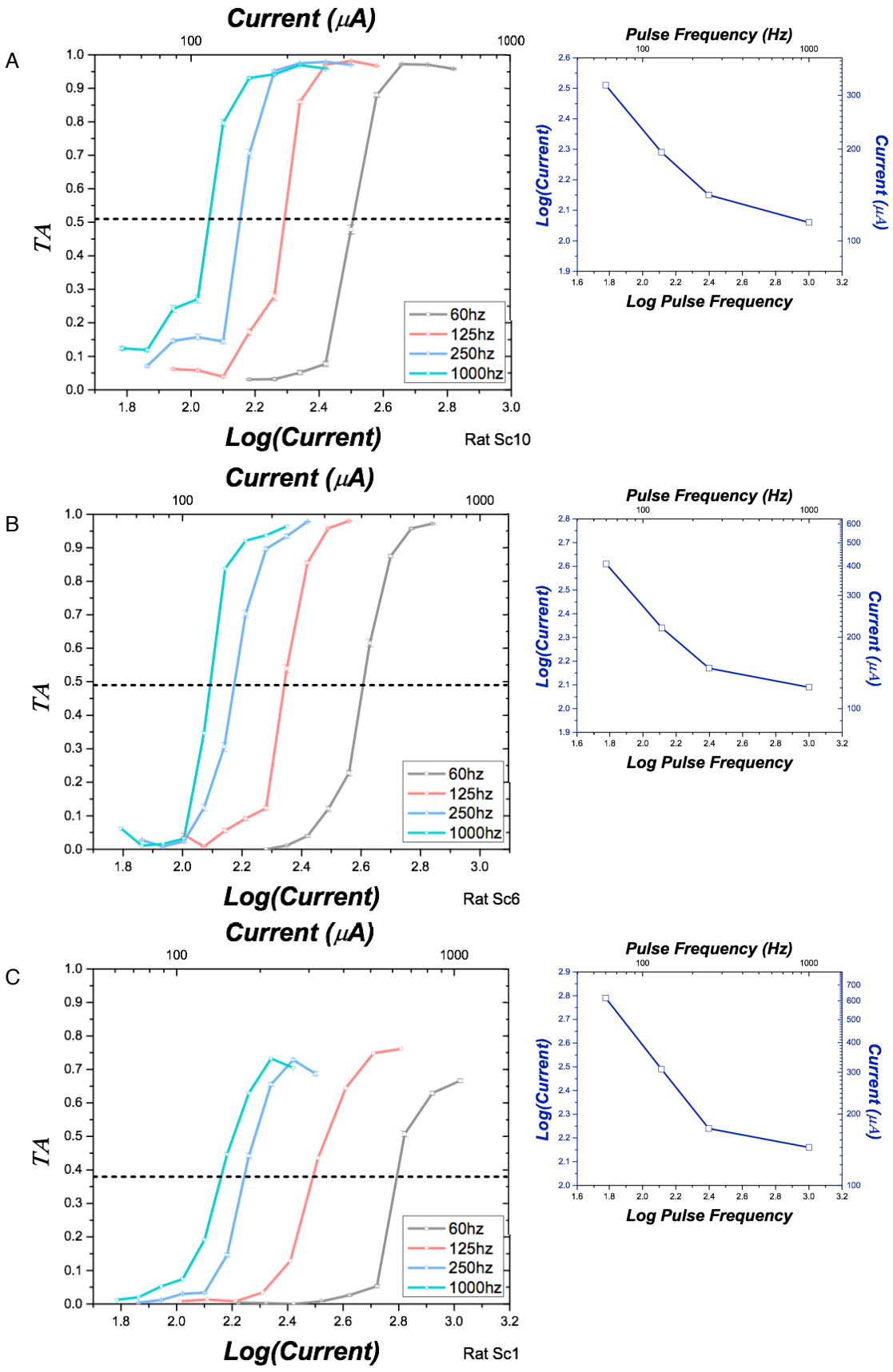
A
Current (μA)
100
1000
TA
Log(Current)
60hz
125hz
250hz
1000hz
Rat Sc10
Pulse Frequency (Hz)
Log(Current)
Current (μA)
Log Pulse Frequency
B
Current (μA)
Rat Sc6
Pulse Frequency (Hz)
Log(Current)
Current (μA)
Log Pulse Frequency
C
Current (μA)
Rat Sc1
Pulse Frequency (Hz)
Log(Current)
Current (μA)
Log Pulse Frequency

D

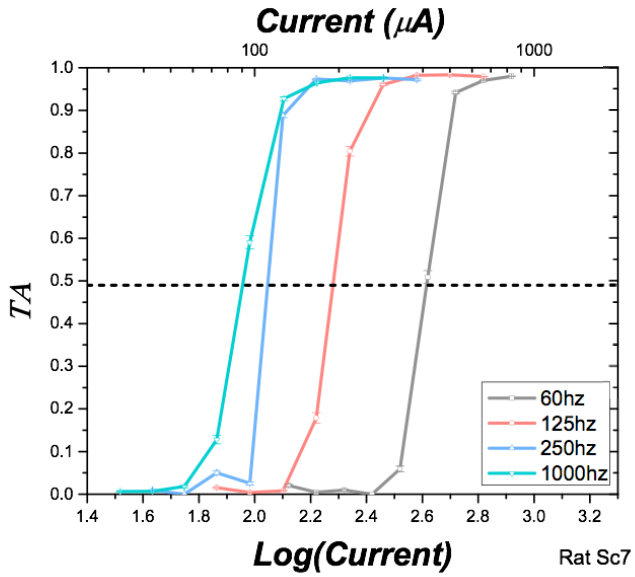
Current (μA)
100
1000
TA
Log(Current)
60hz
125hz
250hz
1000hz
Rat Sc7

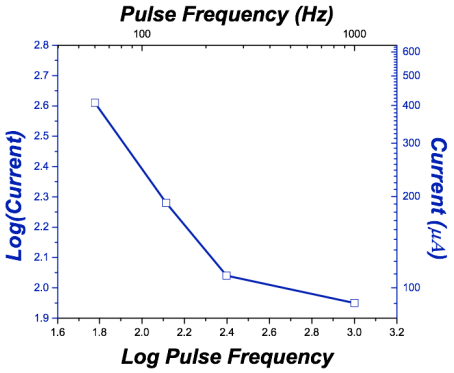
Pulse Frequency (Hz)
100
1000
Log(Current)
Current (μA)
Log Pulse Frequency

E

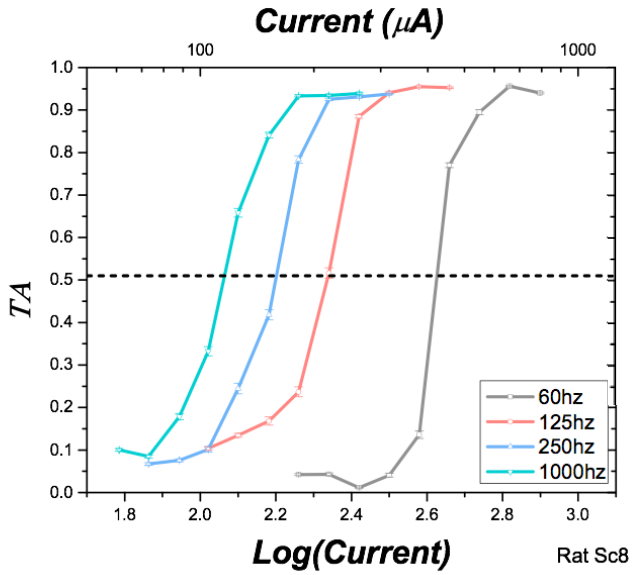
Current (μA)
100
1000
TA
Log(Current)
60hz
125hz
250hz
1000hz
Rat Sc8

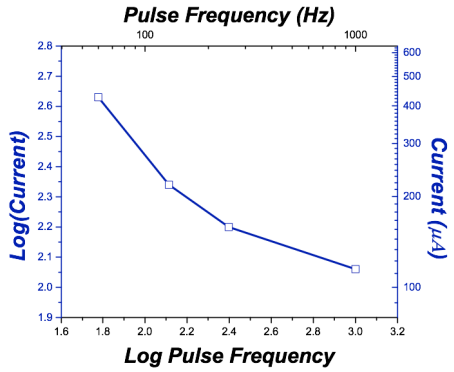
Pulse Frequency (Hz)
100
1000
Log(Current)
Current (μA)
Log Pulse Frequency

Figure 15. Psychometric functions and trade-off functions derived from them. Left-hand panels: Sigmoidal curves relating time allocation to the common logarithm of the current. The dashed horizontal line represents the criterion (the mid-point between the maximal and minimal time allocation) used to derive the trade-off functions. Right-hand panels: Trade-off functions showing the current required to maintain half-maximal time allocation as a function of the pulse frequency. The trade-off functions decline monotonically over the tested range of pulse frequencies.

logarithmic plot decreased over the final increment, from 250 to 1000 Hz (Figure 15). In 4 of 5 rats, the double logarithmic plot of the trade-off function declined linearly, or nearly so, from 60-250 Hz. This means that roughly equal proportional increments in current offset roughly equal proportional increments in pulse frequency. In no case did the trade-off functions level off or begin to rise throughout the tested range of pulse frequencies.

Neurochemical response to MFB stimulation

All DA transients were time-locked to the stimulation trains and all voltammograms had a signature characteristic of DA, with a peak oxidation at roughly 0.6 V and a reduction peak at -0.2 V. The quality of the signature was comparable at all pulse frequencies. In most cases, changes in DA levels lasted between 2 to 3 s (see Figure 16 to 18). Together, these observations indicate that recording sites were located in the vicinity of DA terminals and that clear voltammetric signals were successfully obtained at all pulse frequencies.

Chemometric functions

The curves in the left-hand panels of Figure 19 relate the peak amplitude of stimulation-evoked DA transients in the NAc to the stimulation current. By analogy to the

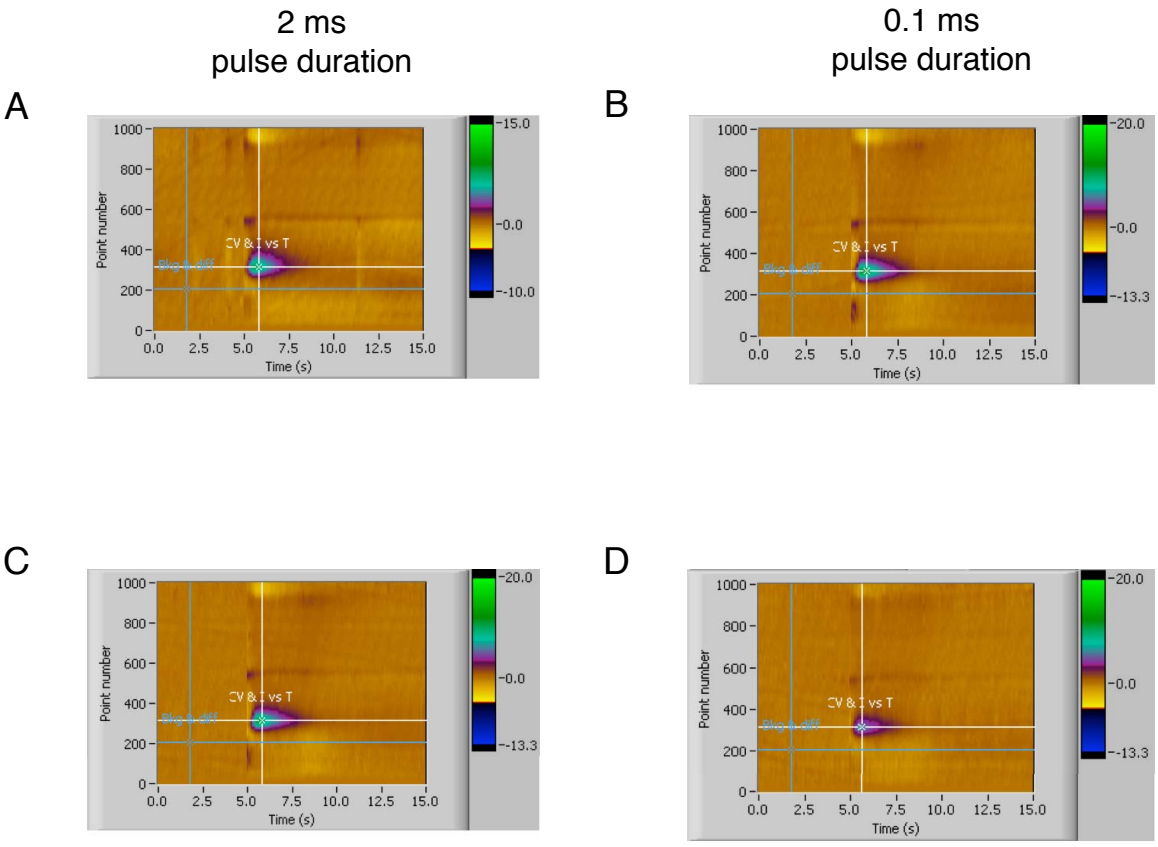

Figure 16. Voltammograms from Sc 6. These color plots contain 150 background-subtracted cyclic voltammograms acquired over 15 s. The changes in voltammetric current are expressed as a function of time (s) on the x axis and point number on the y axis, representing the potentials applied at the carbon fiber at each scan. These false-color voltammograms were obtained at a stimulation current of 691 µA and a pulse frequency of A) 60 Hz, B) 130 Hz, C) 250 Hz and D) 1000 Hz.

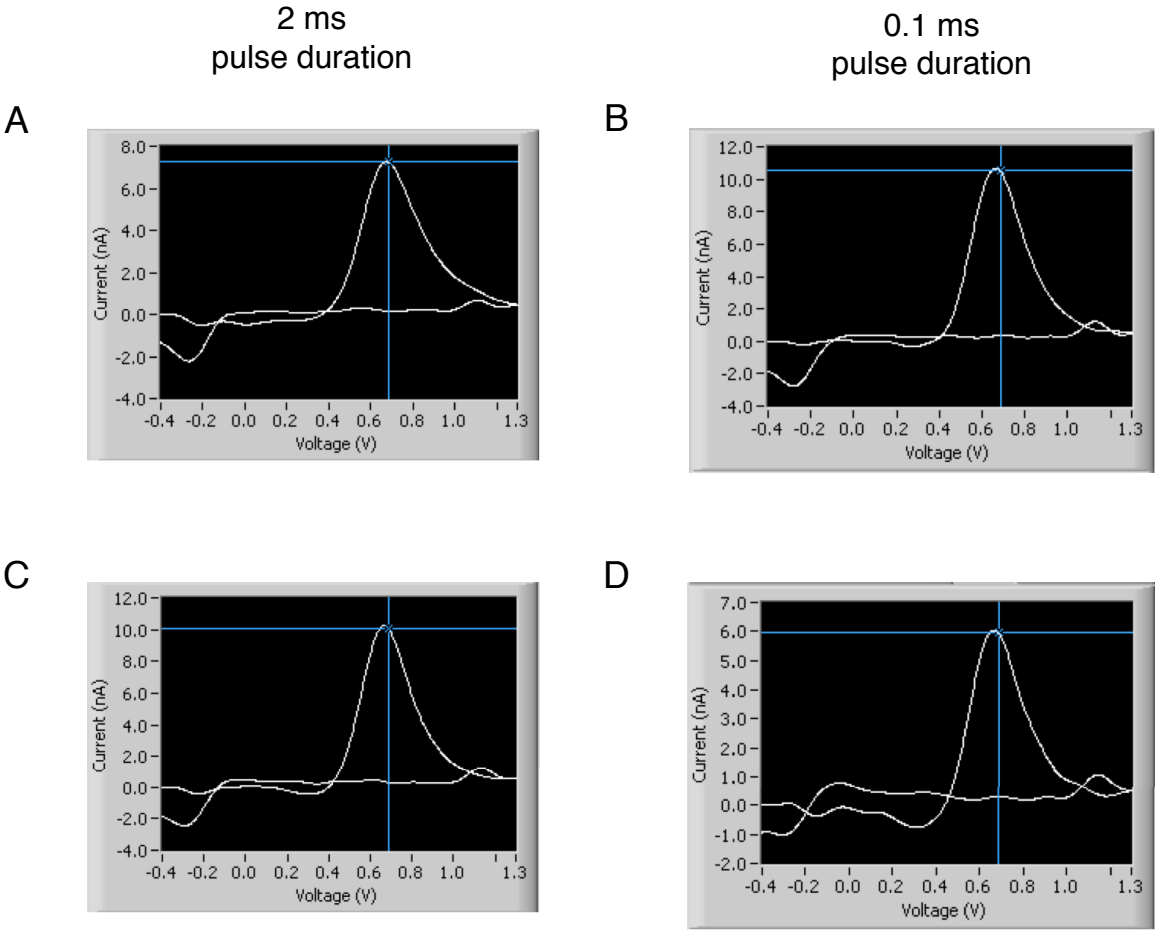

Figure 17. Cyclic voltammetry signatures from Sc 6. These graphs correspond to vertical cross-sections of the false-color voltammographs such as those presented in Figure 5. These traces represent changes in voltammetric current as a function of potential applied at the carbon fiber for the point in time when DA concentration was maximal. A peak oxidation is observed at roughly 0.6 V and a reduction peak at -0.2 V. The signatures were obtained at a stimulation current of 691 µA and a pulse frequency of A) 60 Hz, B) 130 Hz, C) 250 Hz and D) 1000 Hz.

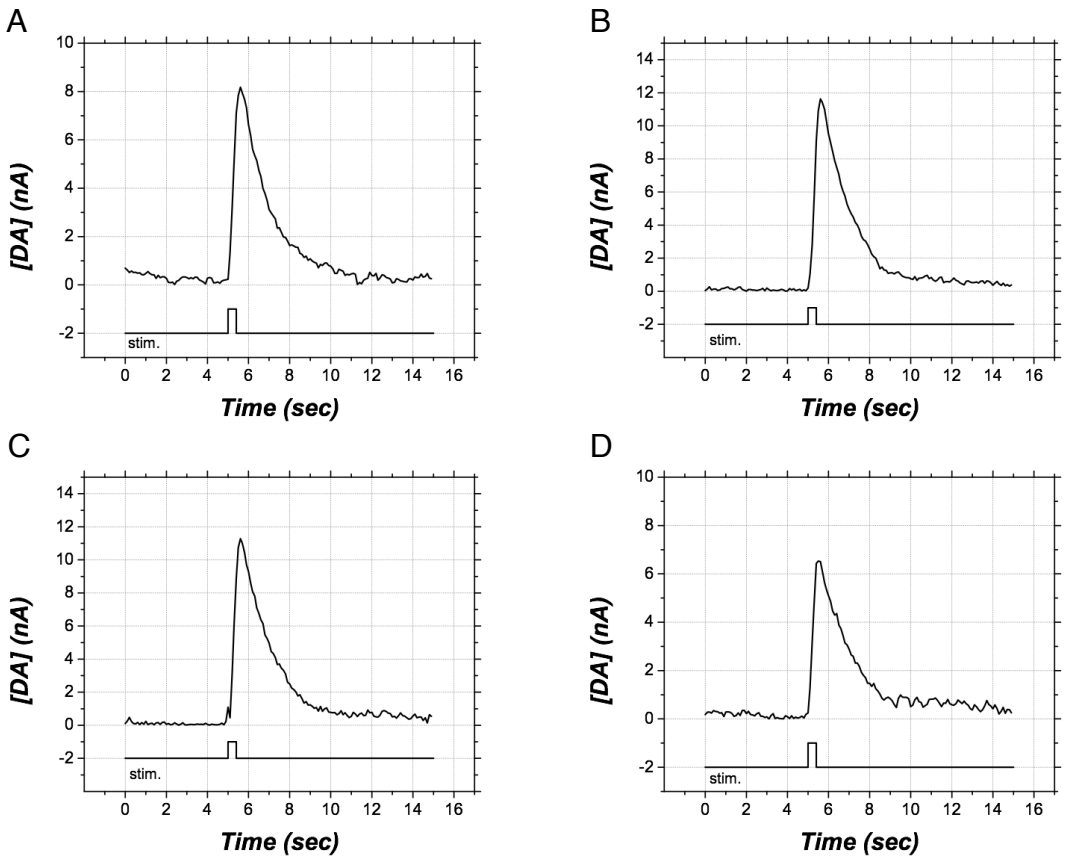

Figure 18. DA transients in response to MFB stimulation. Representative voltammetric traces for rat Sc 6. These graphs correspond to horizontal cross-sections of the false-color voltammograms such as those presented in Figure 16. These traces represent voltammetric changes as a function of time (s) for the potential at which DA concentration was maximal. The traces were obtained at a stimulation current of 691 μA and a pulse frequency of A) 60 Hz, B) 130 Hz, C) 250 Hz and D) 1000 Hz. The stimulation was delivered 5 s after the onset of each voltammetric recording.

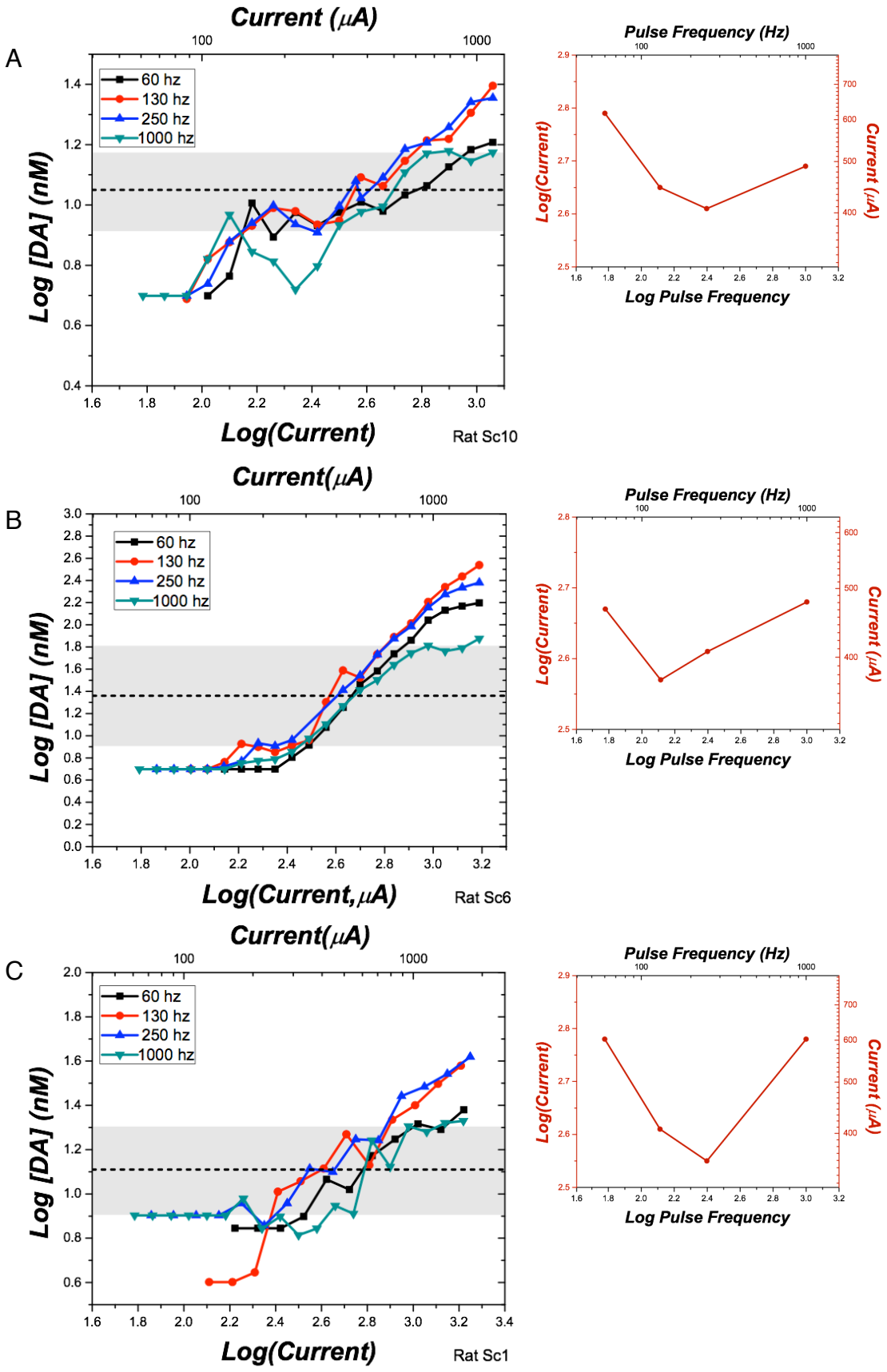
A
Current (μA)
100
1000
60 hz
130 hz
250 hz
1000 hz
Log [DA] (nM)
Log(Current)
Rat Sc10
Pulse Frequency (Hz)
Log(Current)
Current (μA)
Log Pulse Frequency
B
Current(μA)
Log(Current,μA)
Rat Sc6
C
Rat Sc1

D

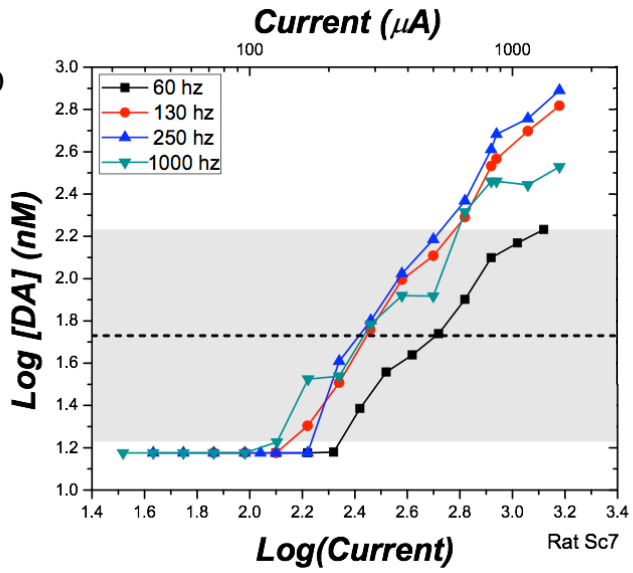
Current (μA)
100
1000
60 hz
130 hz
250 hz
1000 hz
Log [DA] (nM)
Log(Current)
Rat Sc7

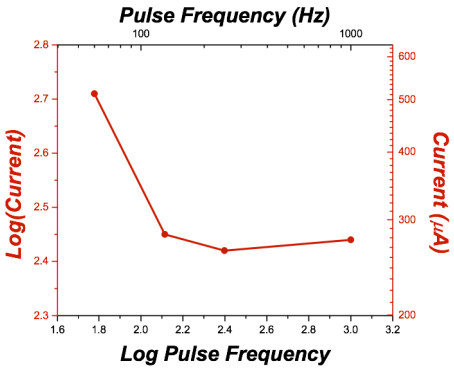
Pulse Frequency (Hz)
100
1000
Log(Current)
Current (μA)
Log Pulse Frequency

E

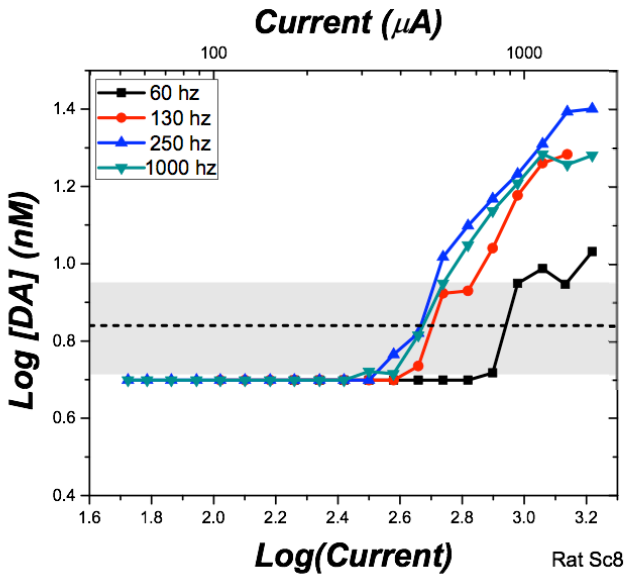
Current (μA)
100
1000
60 hz
130 hz
250 hz
1000 hz
Log [DA] (nM)
Log(Current)
Rat Sc8

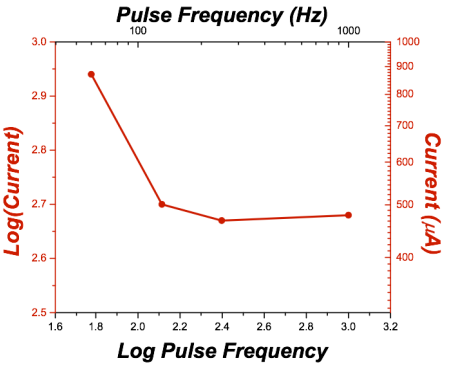
Pulse Frequency (Hz)
100
1000
Log(Current)
Current (μA)
Log Pulse Frequency

Figure 19. Chemometric functions and the trade-off functions derived from them. Left-hand panels: Peak DA oxidation currents as a function of current and pulse frequency. The grey shaded area represents the quasi-linear portion of the growth in the amplitude of the DA transients represented by the rightmost curve. The dashed horizontal line denotes the mid-point of the range in DA concentrations highlighted by the grey shaded area. The values represented by the dashed horizontal lines served as the criterion for deriving the trade-off functions. Right-hand panels: Trade-off functions representing changes in the current required to produce a DA transient of criterial amplitude as a function of pulse frequency. The trade-off functions decline as the pulse frequency is increased from 60 to 130 Hz. Subsequent increases in pulse frequency resulted in either a levelling off of the trade-off curve or a rise.

psychometric curves in the left-hand panels of Figure 15, the curves in the left-hand panels of Figure 19 will be called “chemometric.” Over at least a substantial portion of the current range, the DA transients grew quasi-linearly as a function of current in the double logarithmic plots. Over these portions of the current range, equal proportional increments in current yielded corresponding proportional increments in the peak DA oxidation current.

Changing the pulse frequency produced at least some dispersion of the chemometric curves, but the effect was smaller and less systematic than in the case of the psychometric curves. The effect of changing the pulse frequency is described by the trade-off functions in the right-hand panels of Figure 19. As a function of the pulse frequency, these trade-off functions plot the current required to produce a DA transient of criterial amplitude. In preparation for drawing the trade-off functions, the portion of the rightmost curve that grew quasi-linearly was identified by visual inspection (the grey shaded area in the left-hand panels of Figure 19). The dashed horizontal line in the left-hand panels denotes the mid-point of the amplitude range spanned by the shaded region, the value used to derive the trade-off functions in the right-hand panels of Figure 19. In all rats, the trade-off function declined when the pulse frequency was increased from 60 to 130 Hz. However, subsequent increases in pulse frequency resulted in either a levelling off of the trade-off curve or a rise.

The comparison between behavioural and neurochemical measurements

Figure 20 replots the trade-off functions derived from the psychometric curves in

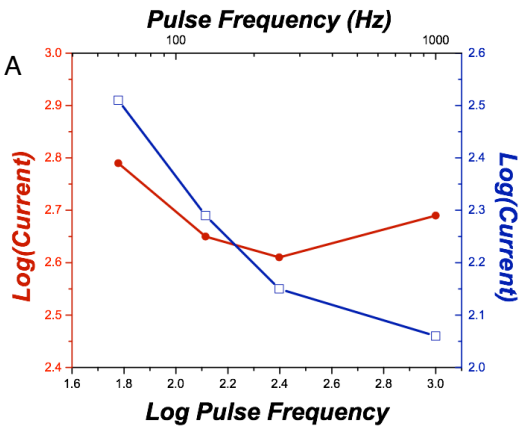
A
Pulse Frequency (Hz)
100
1000
Log(Current)
Log(Current)
Log Pulse Frequency

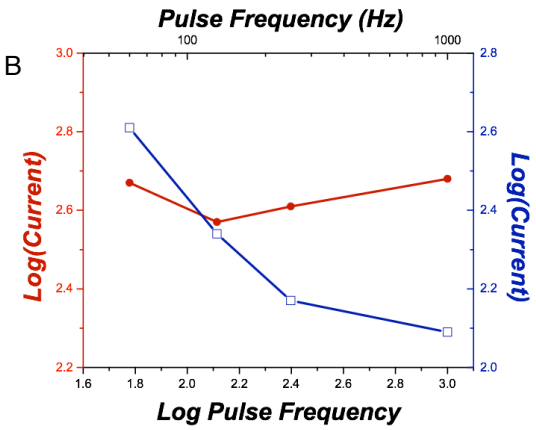
B
Pulse Frequency (Hz)
100
1000
Log(Current)
Log(Current)
Log Pulse Frequency

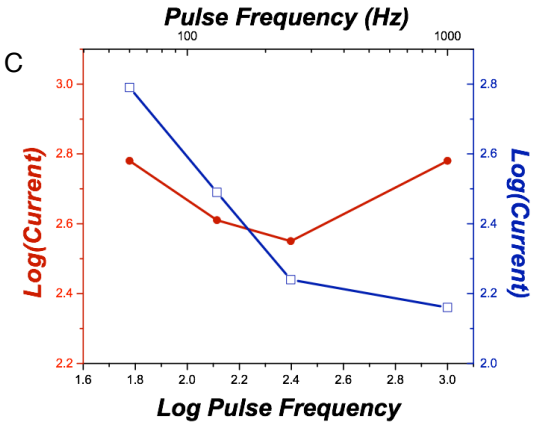
C
Pulse Frequency (Hz)
100
1000
Log(Current)
Log(Current)
Log Pulse Frequency

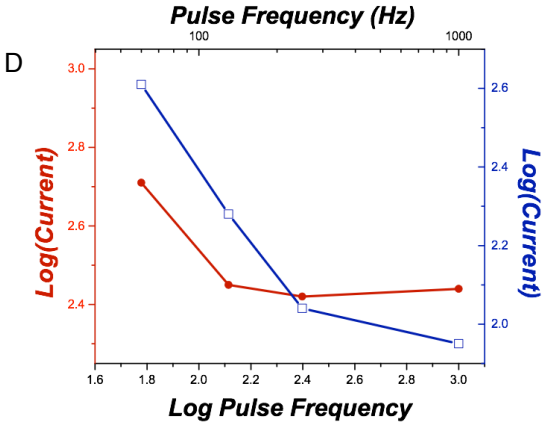
D
Pulse Frequency (Hz)
100
1000
Log(Current)
Log(Current)
Log Pulse Frequency

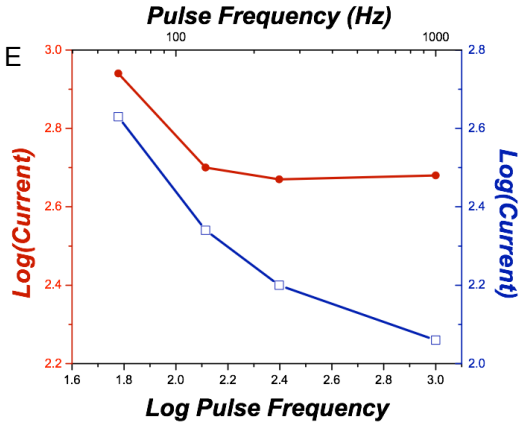
E
Pulse Frequency (Hz)
100
1000
Log(Current)
Log(Current)
Log Pulse Frequency

Figure 20. Comparison between behavioural and neurochemical trade-off functions. For all rats included in the study (A-E), the trade-off functions derived from the psychometric curves (blue open squares) in Figure 15 and from the chemometric curves (red filled circles) in Figure 19 did not match. The trade-off functions for the behavioural data decline monotonically over the tested range of frequencies but the slopes of the chemometric data either change sign (panels A-C) or level off as the pulse frequency is increased.

Figure 15 and the chemometric curves in Figure 19 so as to facilitate comparison. The contrast is striking. Whereas the trade-off functions for the behavioural data (blue) decline systematically, the slopes of the chemometric data (red) either change sign (panels A-C) or level off (panels D,E) as the pulse frequency is increased. The levelling off of the chemometric trade-off functions in panels D and E begins at 130 Hz whereas all the psychometric trade-off functions decline sharply between 130 and 250 Hz. Although the chemometric trade-off functions track their psychophysical counterparts over the lowest portion of the pulse-frequency range, the two functions diverge quite dramatically as the pulse frequency is increased beyond 130 Hz.

DISCUSSION

The reward efficiency of MFB stimulation depends on the spatio-temporal integration of the overall number of action potentials generated at the tip of the electrode (Gallistel, 1978; Simmons & Gallistel, 1994; Gallistel et al., 1981). The number of action potentials per neuron is determined by the pulse frequency whereas the number of stimulated neurons is determined by the current (Gallistel et al., 1981). Therefore, increases in pulse frequency can offset decreases in current so as to hold reward efficacy constant. Consistent with this view, the psychophysical curves obtained in this experiment shifted systematically leftward as the pulse frequency was increased; lower currents were required to sustain ICSS at higher pulse frequencies.

The current-frequency trade-off functions decline monotonically over the tested range of pulse frequencies. Between 60 and 250 Hz, this decline is linear in the double logarithmic plot, or nearly so, in 4 of the 5 cases. This proportionality between pulse frequency and current is consistent with the spatio-temporal integration of impulse flow at the early stage of reward valuation, a proportionality that should be reflected by any other neural elements in series as part of the reward circuitry translating the aggregate impulse flow to the level of performance for ICSS (Gallistel et al., 1981).

In all cases, the slope of the current-frequency trade-off function derived from the psychometric curves declined as the pulse frequency increased from 250 to 1000 Hz. This deceleration is consistent with the high-frequency roll-off in the frequency response of the ICSS substrate posited by Gallistel (1978). The roll-off is attributed to some combination of two phenomena: a progressive failure of the directly stimulated neurons

to fire an action potential in response to each stimulation pulse, and fatigue in synaptic transmission. The resulting saturation of the response of the ICSS substrate is expressed as progressively smaller leftward shifts in the psychophysical curves are observed as the pulse frequency is increased within the roll-off range. (Simmons & Gallistel, 1994; Solomon et al., 2010).

Moisan and Rompré (1998) proposed that midbrain DA neurons are implicated in integrating the aggregate impulse flow produced at the tip of the MFB electrode or constitute a downstream series element that relays this integrated reward signal to efferent stages of the reward circuitry. This hypothesis predicts that some aspect of the activity of the DA neurons tracks the form of trade-off functions reflecting the inter-relationship of the variables that determine aggregate impulse flow in the directly stimulated stage of the ICSS substrate (Gallistel et al., 1981).

As would be expected if DA transients reflected aggregate impulse flow in the ICSS substrate, peak oxidation current grew as a function of the stimulation current. However, leftward displacements of the chemometric curves were observed consistently only from 60 to 130 Hz. Subsequent increases in pulse frequency either failed to displace the curves leftward or resulted in rightward displacements. Thus, the trade-off functions that summarise the effect of varying pulse frequency on the chemometric curves decrease initially but then either rise back towards the value obtained at 60 Hz or flatten. This pattern diverges sharply from the monotonic decline of the trade-off functions derived from the psychometric curves (Figure 20).

The divergence of the trade-off functions derived from the behavioural and neurochemical data is problematic for Moisan & Rompré's hypothesis. If DA neurons

integrate the post-synaptic effects of the stimulation-induced excitation of the directly stimulated neurons subserving ICSS or relay the reward signal to subsequent stages of the circuitry subserving the rewarding effect, then the output of these neurons must reflect the current-frequency trade-off function for ICSS. Otherwise, this relationship, which is due exclusively or largely to events in the directly stimulated stage, could not be manifested in the final behavioural output.

The Moisan and Rompré hypothesis pertains to a population property of the DA neurons. However, DA detection by means of FSCV is restricted to the vicinity of the carbon-fiber electrode and, presumably represents only a small proportion of the DA projection to the NAc terminal field. Thus, to evaluate the Moisan and Rompré hypothesis, we must examine how local responses could be combined to yield a population response integrated across the terminal field.

Although none of the local DA responses measured in the present experiment track the trade-off function derived from the behavioural data, could the entire set of local responses do the job collectively? In principle, a subset of DA neurons could track changes in aggregate impulse flow only over the low-frequency portion of the range, another subset of DA neurons would be responsible for the intermediate frequencies and yet another for the highest frequencies. In that case, the aggregate impulse flow could be reconstituted by integrating local DA responses over the terminal field. There are two problems with this idea. First, it not obvious how the bandpass filtration would be achieved so as to map different portions of the pulse-frequency range onto activation of different “micro-domains” in the ventral striatum, and we know of no data suggesting that such frequency-dependent filtration occurs. A second and far more serious problem

is that none of the recorded transients track the steady decline in the behaviourally derived current-frequency trade-off function beyond 130 Hz, and that several of the trade-off functions derived from the chemometric data have the wrong sign over at least some portion of the tested range. There is no straightforward way to combine the individual sets of neurochemical responses to produce a trade-off function resembling the one derived from the behaviour of the self-stimulating rats. Thus, in order for the Moisan and Rompré hypothesis to be correct, it would have to describe DA release in a region other than one from which the present recordings were obtained, and it would have to be modified to somehow exclude the micro-domains exhibiting U-shaped trade-off functions from the integrated reward signal.

The findings of the present study are in line with those reported by Miliaressis et al. (1991) who measured tonic DA levels in the NAc in response to MFB stimulation using microdialysis. They obtained psychometric curves relating response rates to currents at different pulse durations and derived trade-off function by selecting combinations of stimulation parameters that sustained a 75% maximal response rate. In response to stimulation at parameters sampled along the trade-off function, DA levels decreased as a function of pulse duration, instead of remaining constant. Again, the valence of changes in DA release was opposite to the one predicted by the trade-off function obtained from ICSS performance. As in the present study, there is no simple way to reconstitute reward effectiveness as derived from the behavioural data by integrating the measured changes in NAc DA release.

Monotonic increase in fast and slow DA release concurrent to increase in stimulation parameters that affect reward effectiveness (e.g., pulse frequency, current,

pulse duration or train duration) have been described in several instances (Fiorino et al., 1993, Gratton et al., 1988; Blaha & Phillips, 1990; Gonon, 1988, Wightman et al., 1988; Kawagoe et al., 1994; Garris & Rebec, 2002, Beyene et al., 2010). Results from these experiments have been interpreted as consistent with the notion that DA neurotransmission tracks reward magnitude. However, the tests performed in these studies are not demanding ones because the range of stimulation strengths tested was modest and was not shown to extend into the regions in which behaviourally derived trade-off functions bend. To put the hypothesis to a strong test, a large range of currents and frequencies must be tested. The present study demonstrates that when the range of stimulation parameters is suitably extended, trade-off functions derived from neurochemical measurements of DA levels diverge sharply from those derived from behavioural measurements obtained in self-stimulating rats. No simple scheme is apparent that could combine and transform the neurochemical data so as to produce trade-off functions resembling the ones derived from the psychometric curves.

A caveat must be attached to the interpretation of the data because the neurochemical results were obtained in anaesthetised subjects. One cannot rule out the possibility that the form of the trade-off functions derived from the chemometric data was affected by anaesthesia. Therefore, it will be important to repeat this experiment, substituting FSCV recording in behaving subjects (Clark, Sandberg, Wanat et al., 2010) for the recordings in anaesthetised subjects reported here.

This caveat concerning anaesthesia notwithstanding, the results of this study argue that the role of fast DA neurotransmission in ICSS remains to be elucidated.

GENERAL DISCUSSION

The experiments described in this thesis investigate the transient release of DA in response to rewarding MFB stimulation. This work addresses the circuitry linking the stimulation electrode to DA cell bodies in the VTA and the role of projections from VTA DA neurons to the NAc shell in the rewarding effect of the MFB stimulation.

Although the axons of DA fibers course through ICSS sites along the MFB (Ungerstedt, 1971), non-DA neurons are recruited by the MFB stimulation (Rompré & Shizgal, 1986; Shizgal et al., 1989; Murray & Shizgal, 1996). Some of the latter neurons provide monosynaptic or disynaptic input to the DA cell bodies. As a result, there are numerous ways in which midbrain DA neurons can be activated during self-stimulation of the MFB. Experiment 1 takes advantage of the fact that midbrain DA projections are overwhelmingly unilateral (Lindvall & Björklund, 1974; Swanson, 1982; Ikemoto, 2007), but that MFB stimulation produces bilateral increases in tonic measures of DA activation (Phillips et al., 1987; Garrigues & Cazala, 1983; Nakahara, et al., 1992) Thus, DA transients in the NAc ipsilateral to the stimulation site could reflect a combination of direct recruitment of DA axons and trans-synaptic DA activation, whereas DA transients in the contralateral NAc would appear to arise exclusively from trans-synaptic DA activation.

Rewarding MFB stimulation triggered DA transients in both hemispheres, and the threshold currents for producing detectable DA transients were similar. However, DA transients grew more steeply as a function of current in the ipsilateral than in the

contralateral NAc, a result consistent with the greater diversity of available routes for activating DA cell bodies by means of ipsilateral, as opposed to contralateral, stimulation. In the context of the known anatomy of DA projections, this result suggests that the trans-synaptic routes are an important source of ipsilateral DA activation and the sole source of contralateral activation. The high correlation, across stimulation sites, between the thresholds for ipsilateral and contralateral activation suggests that the same non-DA subpopulation is responsible for the indirect activation of DA neurons in both hemispheres by near-threshold currents.

The contribution of directly activated, non-DA neurons to excitation of DA neurons by MFB stimulation has often been neglected. Consequently, the results of Experiment 1 argue for a shift of perspective on the circuitry linking MFB reward sites to midbrain DA neurons. These results point the spotlight on glutamatergic and cholinergic neurons that have the anatomical properties necessary for monosynaptic and disynaptic activation of VTA DA neurons. (Chergui et al., 1993; Overton & Clark, 1992; Forster & Blaha, 2000; You et al., 2001; Grace, et al., 2007; Sombers, et al., 2009, Herberg & Rose, 1990; Yeomans et al., 1985; Yeomans et al., 1997; Yeomans et al., 2000, Yeomans et al., 2001; Satoh & Fibiger, 1986; Steinenger et al., 1992; Semba & Fibiger, 1992; Geisler et al., 2007). Optogenetic experiments, such as those sketched out in detail in the discussion of Experiment 1, can provide a powerful way to assess the roles of glutamatergic and cholinergic neurons in the trans-synaptic activation of VTA DA neurons by rewarding MFB stimulation.

In Experiment 1, behavioural testing was used to ensure that the stimulation that

drove the DA transients was, in fact, rewarding. In Experiment 2, the role of the behavioural data was expanded so as to shed light on the role of phasic DA activity in the rewarding effect of MFB stimulation. This was accomplished by determining the trade-off between the stimulation current and the pulse frequency, using both behavioural and neurochemical end points.

Neurons involved in early stages of the neural circuitry subserving the rewarding effect of the MFB stimulation derive the intensity of the reward signal from the overall number of action potentials triggered by a stimulation train. The reward-related circuitry that integrates the post-synaptic effects of the induced volley of action potentials acts as if to count the spikes in the volley. (Gallistel, 1978; Simmons & Gallistel, 1994; Gallistel et al., 1981). Thus, there is a reciprocal relationship between the number of neurons that must be stimulated directly to produce a given level of performance and the frequency at which these neurons are fired by the stimulation. Given the evidence that the different neural stages that translate the stimulation-induced volley into observable operant performance have monotonic input-output functions (Gallistel et al., 1981), the reciprocity between the stimulation current and pulse frequency in maintaining a given rate of aggregate impulse flow in the directly stimulated neurons must also be expressed at the behavioural output, and the current required to sustain a given level of performance must trade off in a scalar (Gallistel et al., 1974; Gallistel, 1978) or linear (Forgie & Shizgal, 1993) manner. If phasic firing in midbrain DA neurons integrates the post-synaptic effect of the stimulation-induced volley or relays the integrated reward signal to efferent stages of the pathway subserving ICSS, then a similar trade-off function must

describe the relationship between current and pulse frequency in driving transient release of DA.

Psychometric functions were obtained relating time allocation, the proportion of trial time the animal works for the electrical stimulation, to the stimulation current. Chemometric functions were obtained to describe how the amplitude of DA transients recorded in the shell region of the NAc grew as a function of stimulation currents delivered by the same electrodes employed in the behavioural phase of the study. These procedures were repeated at four different pulse frequencies. The psychometric curves shifted systematically leftward as the pulse frequency was increased. Thus, the trade-off functions derived from these data declined monotonically. In contrast, the chemometric curves shifted leftward only over the low-frequency portion of the tested range; as the pulse frequency was pushed to higher values, these curves either ceased to shift or moved rightward. The trade-off functions derived from them are either non-monotonic or level off. Thus, the monotonic form of the trade-off functions derived from the behavioural data was not mirrored by the trade-off functions derived from the chemometric data. There is no obvious and straightforward way to combine the individual chemometric trade-off functions so as to produce a result that resembles the behaviourally derived trade-off functions. This is inconsistent with the hypothesis that VTA DA neurons projecting to the NAc shell constitute an entire series stage of the circuit responsible for the rewarding effect of the MFB stimulation.

DA transients have been described as sensitive to reward magnitude (Beyene et al., 2010). However, simply demonstrating that the transients grow as a function of a

stimulation parameter that increases ICSS performance is not a demanding test of this notion. Indeed, all of the chemometic functions obtained in Experiment 2 rise over some range of currents. However, by examining how these functions are altered by changes in pulse frequency, Experiment 2 demonstrates an important discrepancy between the characteristics of the DA transients and those required to account for the behaviourally derived trade-off between current and pulse frequency. Thus, the exact role of phasic DA activity in reward processing, and in MFB self-stimulation in particular, remains to be determined.

One goal of the work reported here was to provide a foundation for experiments that can identify the directly activated neurons underlying the rewarding effect of MFB stimulation, determine how these neurons interact with VTA DA neurons, and clarify how the DA neurons contribute to ICSS. An important next step is to repeat the neurochemical measurements in behaving rats so as to determine whether anesthesia contributed to the discrepancy between the trade-off functions derived from the behavioural and neurochemical data.

The self-stimulation phenomenon is a powerful tool for probing brain reward circuitry and is believed to arise from activation of neural circuitry that is also involved in the pursuit of naturally-occurring and drug-induced rewards (Wise, 2004; Ikemoto, 2010). Achieving a better understanding of the anatomical and functional basis of ICSS promises to shed light on a wide variety of reward seeking behaviours and perhaps on the ways in which these behaviours can become dysfunctional.

Rat No.	Ratio of slopes for linear fits (ipsi/contra)	
	2 ms pulse duration	0.1 ms pulse duration
IC 1	1.68	1.56
IC 2	1.18	1.19
IC 3	1.93	2.11
IC 4	3.23	1.58
IC 5	0.83	0.61
IC 6	2.29	1.71
IC 7	2.25	1.52

Figure 1. Growth in DA transients. Ratio of slopes from linear fits relating peak DA concentration as a function of current.

REFERENCES

Arvanitogiannis, A., Flores, C., Pfaus, J. G. & Shizgal, P. (1996). Increased ipsilateral expression of Fos following lateral hypothalamic self-stimulation. *Brain research*, *720(1-2)*, 148-54.

Beyene, M. (2009) *Pasic dopamine release: its origin and function in reward seeking* (Doctoral dissertation) Retrieved from http://www.lib.unc.edu.

Beyene, M., Carelli, R. M. & Wightman, R M. (2010). Cue-evoked dopamine release in the nucleus accumbens shell tracks reinforcer magnitude during intracranial self-stimulation. *Neuroscience*, *169(4)*, 1682-8.

Bernard, V., Legay, C., Massoulie, J. & Bloch, B. (1995) Anatomical analysis of the neurons expressing the acetylcholinesterase gene in the rat brain, with special reference to the striatum. *Neuroscience, 64(4),* 995-1005.

Bielajew, C. & Shizgal, P. (1982). Behaviorally derived measures of conduction velocity in the substrate for rewarding medial forebrain bundle stimulation. *Brain research*, *237*, 107-119.

Bielajew, C. & Shizgal, P. (1986). Evidence implicating descending fibers in self-stimulation of the medial forebrain bundle, *The Journal of neuroscience, 6(4)*, 919-929.

Björklund, A. & Dunnett, S. B. (2007). Dopamine neuron systems in the brain: an update. *Trends in neurosciences*, *30(5)*, 194-202.

Blaha, C. D. & Phillips, A. G. (1990) Application of in vivo electrochemistry to the measurement of changes in dopamine release during intracranial self-stimulation. *Journal of neuroscience Methods, 34,* 125-133.

Blaha, C. D. & Phillips, A. G. (1996) A critical assessment of electrochemical procedures applied to the measurement of dopamine and its metabolites during drug-induced and species-typical behaviours. *Behavioural pharmacology, 7,* 675-708.

Boyden, E., S. Zhang, F., Bamberg, E., Nagel, G. & Deisseroth, K. (2005) Millisecond-timescale, genetically targeted optical control of neural activity. *Nature Neuroscience, 8(9),* 1263-1268.

Breton, Y.-A., Marcus, J. C. & Shizgal, P. (2009). Rattus Psychologicus: construction of preferences by self-stimulating rats. *Behavioural brain research*, *202(1)*, 77-91.

Cheer, J. F., Heien, M. L., Garris, P. A., Carelli, R. M. & Wightman, R Mark. (2005). Simultaneous dopamine and single-unit recordings reveal accumbens GABAergic responses: implications for intracranial self-stimulation. *PNAS, 102 (52),* 19150-19155.

Clark, J. J., Sandberg, S. G., Wanat, M. J., Gan, J. O., Hart, A. S., Akers, C. A., Parker, J. G., Willuhn, I., Martinez. V., Evans, S. B., Stella, N. & Phillips, P. E. (2010). Chronic microsensors for longitudinal, subsecond dopamine detection in behaving animals, *Nature Methods, 7(2)*, 126-129.

Chergui, K., Charlety, P. J., Akaoka, H., Saunier, C. F., Brunet, J. L., Buda, M., Svensson, T. H. & Chouvet, G. (1993). Tonic activation of NMDA receptors

causes spontaneous burst discharge of rat midbrain dopamine neurons in vivo. *The European journal of neuroscience*, *5(2)*, 137-44.

Conover, K. L., & Shizgal, P. (1994). Competition and summation between rewarding effects of sucrose and lateral hypothalamic stimulation in the rat. *Behavioral neuroscience*, *108(3)*, 537-48.

Conover, K. L., Woodside, B., & Shizgal, P. (1994). Effects of sodium depletion on competition and summation between rewarding effects of salt and lateral hypothalamic stimulation in the rat. *Behavioral neuroscience*, *108(3)*, 549-58.

Corbett, D. & Wise, R. (1980). Intracranial self-stimulation in relation to the ascending dopaminergic systems of the midbrain: a moveable electrode mapping study. *Brain research, 185,* 1-15.

Crow, T. J. (1970). Enhancement by cocaine of intra-cranial self-stimulation in the rat. *Life* science*, 9,* 375-381.

Edmonds, D. E., Stellar. J. R. & Gallistel, C. R. (1974) Parametric analysis of brain stimulation reward in the rat: II. Temporal summation in the reward system. *Journal of comparative and physiological psychology, 87(5),* 860-869.

Fiorino, D. F., Coury, A., Fibiger, H. C. & Phillips, A. G. (1993). Electrical stimulation of reward sites in the ventral tegmental area increases dopamine transmission in the nucleus accumbens of the rat. *Behavioural brain research*, *55(2)*, 131-41.

Floresco, S. B., West, A. R., Ash, B., Moore, H. & Grace, A. A. (2003). Afferent modulation of dopamine neuron firing differentially regulates tonic and phasic dopamine transmission. *Nature neuroscience*, *6(9)*, 968-73.

Forgie, M. L. & Shizgal, P. (1993) Mapping the substrate for brain stimulation reward by means of current-number trade-off functions. *Behavioral Neuroscience, 107(3),* 506-524.

Forster, G. L. & Blaha, C. D. (2000). Laterodorsal tegmental stimulation elicits dopamine efflux in the rat nucleus accumbens by activation of acetylcholine and glutamate receptors in the ventral tegmental area. *The European journal of neuroscience*, *12(10)*, 3596-604.

Gallistel, C. R. (1978) Self-stimulation in the rat: quantitative characteristics of the reward pathway. *Journal of comparative and physiological psychology, 92(6),* 977-998.

Gallistel, C. R. & Karras, D. (1984). Pimozide and amphetamine have opposing effects on the reward summation function. *Pharmacology, biochemistry, and behavior*, *20*(1), 73-7.

Gallistel, C. R. & Leon, M. (1991a). Measuring the subjective magnitude of brain stimulation reward by titration with rate of reward. *Behavioral neuroscience*, *105(6)*, 913-25.

Gallistel, C. R. Leon, M., Waraczynski, M. & Hanau, M. S. (1991b). Effect of current on the maximum possible reward. *Behavioral neuroscience*, *105(6)*, 901-12.

Gallistel, C. R. Shizgal, P, & Yeomans, J. S. (1981). A portrait of the substrate for self-stimulation. *Psychological review*, *88(3)*, 228-73.

Garrigues, A. M. & Cazala, P. (1983). Central catecholamine metabolism and hypothalamic self-stimulation behaviour in two inbred strains of mice. *Brain research*, *265(2)*, 265-71.

Garris, P. A., Ciolkowski, E., L., Pastore, P. & Wightman, R. M. (1994) Efflux of dopamine from the synaptic cleft in the nucleus accumbens of the rat brain. *Journal of Neuroscience, 14(10),* 6084-6093.

Garris, P., A. & Rebec, G., V. (2002) Modeling fast dopamine neurotransmission in the nucleus accumbens during behavior. *Behavioural brain research, 137,* 47-63.

Geisler, S., Derst, C., Veh, R. W. & Zahm, D. S. (2007). Glutamatergic afferents of the ventral tegmental area in the rat. *The Journal of neuroscience*, *27(21)*, 5730-43.

German, D. C. & Bowden, D. M. (1974) Catecholamine systems as the neural substrate for intra-cranial self-stimulation: a hypothesis. *Brain research, 73,* 381-419.

Gonon, F. G. (1988). Nonlinear relationship between impulse flow and dopamine released by rat midbrain dopaminergic neurons as studied by in vivo electrochemistry. *Neuroscience*, *24(1)*, 19-28.

Grace, A. A. & Onn, S. P. (1989). Morphology and electrophysiological properties of immunocytochemically identified rat dopamine neurons recorded in vitro. *The Journal of neuroscience*, *9(10)*, 3463-81.

Grace, A. & Bunney, S. (1984a). The control of firing neurons in nigral dopamine neurons: single spike firing. *Journal of Neuroscience*, *4(11)*, 2866-2876.

Grace, A. & Bunney, S. (1984b). The control of firing neurons in nigral dopamine neurons: burst firing. *Journal of Neuroscience*, *4(11)*, 2877-2890.

Grace, A., Floresco, S. B., Goto, Y. & Lodge, D. J. (2007). Regulation of firing of dopaminergic neurons and control of goal-directed behaviors. *Trends in neurosciences*, *30(5)*, 220-7.

Gradinaru, V., Zhang, F., Ramakrishnan, C. Mattis, J. Prakash, R. Diester, I. Goshen, I. Thompson, K., R. & Deisseroth, K. (2010) Molecular and cellular approaches for diversifying and extending optogenetics. *Cell, 141,* 154-165.

Gratton, A., Hoffer B. J. & Gerhardt, G. A. (1988). Effects of electrical stimulation of brain reward sites on release of dopamine in rat: an in vivo electrochemical study. *Brain Research Bulletin*, *21(2)*, 319-324.

Herberg, L. J. & Rose, I. C. (1990). Excitatory amino acid pathways in brain-stimulation reward. *Behavioural brain research*, *39(3)*, 230-9.

Hernandez, G., Breton, Y.-A., Conover, K. & Shizgal, P. (2010). At what stage of neural processing does cocaine act to boost pursuit of rewards? *PloS one*, *5*(11), e15081-e15081.

Hunt, G. E. & McGregor, I. S. (1998). Rewarding brain stimulation induces only sparse Fos-like immunoreactivity in dopaminergic neurons. *Neuroscience*, *83*(2), 501-15.

Hyland, B. I., Reynolds, J. N. J., Hay, J., Perk, C. G. & Miller, R. (2002). Firing modes of midbrain dopamine cells in the freely moving rat. *Neuroscience*, *114*(2), 475-92.

Ikemoto, S. (2007) Dopamine reward circuitry: two projection systems from the ventral midbrain to the nucleus accumbens-olfactory tubercle complex. *Brain research reviews, 56(1),* 27-78.

Ikemoto, S. (2010) Brain reward circuitry beyond the mesolimbic dopamine system: a neurobiological theory. *Neuroscience & biobehavioral Review, 35(2),* 129-150.

Kawagoe, K. T. & Wightman, R. M. (1994). Characterization of amperometry for in vivo measurement of dopamine dynamics in the rat brain. *Talanta*, *41(6)*, 865-74.

Kilpatrick, M. R., Rooney, M. B., Michael, D. J. & Wightman, R M. (2000). Extracellular dopamine dynamics in rat caudate-putamen during experimenter-delivered and intracranial self-stimulation. *Neuroscience*, *96(4)*, 697-706.

Kuhr, W. C, Wightman, R. M. & Rebec, G. V. (1987). Dopaminergic neurons: simultaneous measurements of dopamine release and single-unit activity during stimulation of the medial forebrain bundle. *Brain Research, 418,* 122-128.

Leon, M. & Gallistel, C. R. (1992). The function relating the subjective magnitude of brain stimulation reward to stimulation strength varies with site of stimulation. *Behavioural brain research, 52*, 183-193.

Lindvall, O. & Björklund, A. (1974) The organization of the ascending catecholamine neuron systems in the brain. *Acta physiologica scandinavica, suppl 412,* 1-48.

Maeda, H. and Mogenson, G.J. (1981) A comparison of the effects of electrical stimulation of the lateral and ventromedial hypothalamus on the activity of neurons in ventral tegmental area and substantia nigra. *Brain Research Bulletin*, 7, 283-291.

Miliaressis, E., Emond, C. & Merali, Z. (1991). Re-evaluation of the role of dopamine in intracranial self-stimulation using in vivo microdialysis. *Behavioural brain research*, *46(1)*, 43-8.

Moisan, J. & Rompré, P. P. (1998). Electrophysiological evidence that a subset of midbrain dopamine neurons integrate the reward signal induced by electrical stimulation of the posterior mesencephalon. *Brain research*, *786(1-2)*, 143-52.

Murray, B. & Shizgal, P. (1996). Behavioral measures of conduction velocity and refractory period for reward-relevant axons in the anterior LH and VTA. *Physiology & behavior*, *59(4-5)*, 643-52.

Murray, B. & Shizgal, P. (1994). Evidence implicating both slow- and fast-conducting fibers in the rewarding effect of medial forebrain bundle stimulation. *Behavioural Brain Research*, *63*, 47-60.

Nakahara, D., Fuchikami, K., Ozaki, N., Iwasaki, T. & Nagatsu, T. (1992). Differential effect of self-stimulation on dopamine release and metabolism in the rat medial frontal cortex, nucleus accumbens and striatum studied by in vivo microdialysis. *Brain research*, *574(1-2)*, 164-70.

Nakahara, D., Ishida, Y., Nakamura, M., Kuwahara, I., Todaka, K. & Nishimori, T. (1999). Regional differences in desensitization of c-Fos expression following repeated self-stimulation of the medial forebrain bundle in the rat. *Neuroscience*, *90*(3), 1013-20.

Nakahara, D., Ozaki, N., Kapoor, V. & Nagatsu, T. (1989). The effect of uptake inhibition on dopamine release from the nucleus accumbens of rats during self- or forced stimulation of the medial forebrain bundle: a microdialysis study. *Neuroscience letters*, *104*(1-2), 136-40.

Nieuwenhuys, R., Geeraedts, L. M. & Veening, J. G. (1982) The medial forebrain bundle of the rat. I. General introduction. *Journal of comparative neurology, 206(1),* 49-81.

Oakman, S. a, Faris, P. L., Kerr, P. E., Cozzari, C. & Hartman, B. K. (1995). Distribution of pontomesencephalic cholinergic neurons projecting to substantia nigra differs significantly from those projecting to ventral tegmental area. *Journal of Neuroscience*, *15*(9), 5859-69.

Olds, M. E., & Olds, J. (1963). Approach-avoidance analysis of rat diencephalon. *The Journal of Comparative Neurology*, *120*(2), 259-295.

Overton, P. & Clark, D. (1992). Iontophoretically administered drugs acting at the N-methyl-D-aspartate receptor modulate burst firing in A9 dopamine neurons in the rat. *Synapse*, *10(2)*, 131-40.

Phillips, A. G., Jakubovic, A. & Fibiger, H. C. (1987). Increased in vivo tyrosine hydroxylase activity in rat telencephalon produced by self-stimulation of the ventral tegmental area. *Brain research*, *402(1)*, 109-16.

Pillolla, G., Melis, M., Perra, S., Muntoni, A. L., Gessa, G. L. & Pistis, M. (2007). Medial forebrain bundle stimulation evokes endocannabinoid-mediated modulation of ventral tegmental area dopamine neuron firing in vivo. *Psychopharmacology*, *191(3)*, 843-53.

Rompré, P. P. & Shizgal, P. (1986). Electrophysiological characteristics of neurons in forebrain regions implicated in self-stimulation of the medial forebrain bundle in the rat. *Brain research*, *364(2)*, 338-49.

Satoh, K. & Fibiger, H. C. (1986) Cholinergic neurons of the laterodorsal tegmental nucleus: efferent and afferent connections. *Journal of comparative neurology, 253,* 277-302.

Semba, K. & Fibiger, H. C. (1992) Afferent connections of the laterodorsal and pedunculopontine tegmental nuclei in the rat: a retro- and antero-grade transport and immunohistochemical study. *Journal of comparative neurology, 323,* 387-410.

Shizgal, P. (1997). Neural basis of utility estimation. *Current opinion in neurobiology*, *7(2)*, 198-208.

Shizgal, P., Bielajew, C, Corbett, D., Skelton, R. & Yeomans, J. (1980). Behavioral methods for inferring anatomical linkage between rewarding brain stimulation sites. *Journal of comparative and physiological psychology*, *94(2)*, 227-37.

Shizgal, P, Schindler, D. & Rompré, P. P. (1989). Forebrain neurons driven by rewarding stimulation of the medial forebrain bundle in the rat: comparison of psychophysical and electrophysiological estimates of refractory periods. *Brain research*, *499(2)*, 234-48.

Simmons, J. M. & Gallistel, C. R. (1994). Saturation of subjective reward magnitude as a function of current and pulse frequency. *Behavioral neuroscience*, *108(1)*, 151-60.

Solomon, R., B., Trujillo-Pisanty, I. & Shizgal, P. (2010, November) *The maximal firing frequency of the neurons subserving brain stimulation reward*. Poster presented at the annual meeting of the Society for Neuroscience, San Diego.

Sombers, L., A., Beyene, M., Carelli, R. M & Wightman, R. M. (2009) Synaptic overflow of dopamine in the nucleus accumbens arises from neuronal activity in the ventral tegmental area. *Journal of neuroscience, 29(6),* 1735-1742.

Steininger, T., L., Rye, D., B. & Wainer, B., H. (1992) Afferent projections to the cholinergic pedunculopontine tegmental nucleus and adjacent midbrain extrapyramidal area in the albino rat. I. Retrograde tracing studies. *The journal of comparative neurology, 321,* 515-543.

Suaud-Chagny, M. F., Dugast, C., Chergui, K., Msghina, M. & Gonon, F. (1995) Uptake of dopamine release by impulse flow in the rat mesolimbic and striatal systems in vivo. *Journal of Neurochemistry, 65(6),* 2603-2611.

Swanson, L., W. (1982). The projections of the ventral tegmental area and adjacent regions: a combined fluorescent retrograde tracer and immunofluorescence study in the rat. *Brain research bulletin*, *9(1-6)*, 321-53.

Tukey, J. W. & McLaughlin, D. H. (1963) Less vulnerable confidence and significance procedures for location based on a single sample: Trimming/Winsorization 1. *The indian journal of statistics, Series A, 25(3),* 331-352.

Ungerstedt, U. (1971) Stereotaxic mapping of the monoamine pathways in the rat brain. *Acta physiologica scandinavica, suppl 367,* 1-48.

Veening, J. A., Swanson, Larry W, Cowan, W. M., Nieuwenhuys, R. & Geeraedts L. E., (1982). The medial forebrain bundle of the rat. II. An autoradiographic study of the topography of the major descending and ascending components. *Journal of comparative neurology, 206(1)*, 82-108.

Waraczynski, M., Stellar, J. R., & Gallistel, C. R. (1987). Reward saturation in medial forebrain bundle self-stimulation. *Physiology & behavior*, *41(6)*, 585-93.

Wightman, R. M., Amatore, C., Engstrom, R. C., Hale, P. D., Kristensen, E. W., Kuhr, W. G. & May, L. J. (1988) Real-time charaterization of dopamine oveflow and uptake in the rat striatum. *Neuroscience, 25 (2),* 513-523.

Wise, R. A. (1980) Action of drugs of abuse on brain reward systems. *Pharmacology Biochemistry & Behavior, 13 (suppl. 1),* 213-223.

Wise, R. A. (1978) Catecholamine theories of reward: a critical review. *Brain Research, 152,* 215-247.

Wise, R. A. (2004). Dopamine, learning and motivation. *Nature reviews. Neuroscience*, *5(6)*, 483-94.

Yavich, L. (2000). Patterns of dopamine overflow in mouse nucleus accumbens during intracranial self-stimulation. *Neuroscience Letters*, *293(1)*, 41-44.

Yavich, L. & Tanila, H. (2007). Mechanics of self-stimulation and dopamine release in the nucleus accumbens. *Neuroreport*, *18(12)*, 1271-4.

Yeomans, J. S. (1989). Two substrates for medial forebrain bundle self-stimulation: myelinated axons and dopamine axons. *Neuroscience and biobehavioral reviews*, *13(2-3)*, 91-8.

Yeomans, J. S. & Baptista, M. (1997). Both nicotinic and muscarinic receptors in ventral tegmental area contribute to brain-stimulation reward. *Pharmacology, biochemistry, and behavior*, *57(4)*, 915-21.

Yeomans, J. S., Mathur, A. & Tampakeras, M. (1993) Rewarding brain stimulation: role of tegmental cholinergic neurons that activate dopamine neurons. *Behavioral neuroscience, 107(6),* 1077-1087.

Yeomans, J. S., Kofman, O. & McFarlane, V. (1985) Cholinergic involvement in lateral hypothalamic rewarding brain stimulation. *Brain research, 329,* 19-26.

Yeomans, J. S., Takeuchi, J., Baptista, M., Flynn, D. D., Lepik, K., Nobrega, J., Fulton, J. & Ralph, M. R. (2000). Brain-stimulation reward thresholds raised by an antisense oligonucleotide for the M5 muscarinic receptor infused near dopamine cells. *Journal of Neuroscience*, *20(23)*, 8861-7.

Yeomans, J., Forster, G. & Blaha, C. (2001). M5 muscarinic receptors are needed for slow activation of dopamine neurons and for rewarding brain stimulation. *Life sciences*, *68(22-23)*, 2449-56.

You, Z. B., Chen, Y. Q. & Wise, R. A. (2001). Dopamine and glutamate release in the nucleus accumbens and ventral tegmental area of rat following lateral hypothalamic self-stimulation. *Neuroscience*, *107(4)*, 629-39.